SAND2019-14628C

# Non-contact Density and Thermal Conductivity Measurements of Encased Organic Thin-Films and Thin-Film Explosives

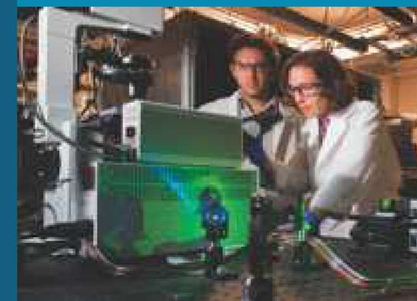

PRESENTED BY

Elbara Ziade

2019-12-02

**Team members:** Chris Perez, Eric Forrest, Michael P. Marquez, Robert Knepper, Alexander S. Tappan

Sandia National Laboratories is a multimission laboratory managed and operated by National Technology and Engineering Solutions of Sandia LLC, a wholly owned subsidiary of Honeywell International Inc. for the U.S. Department of Energy's National Nuclear Security Administration under contract DE-NA0003525.

# Density Measurements of Thin-Films

Thin-film explosives provides us a pathway to fundamentally understand reactive material detonation phenomena. However, the density of thin-film explosives differs from the bulk counterpart and our models depend on accurate density measurements.

**Problem**: Non-destructive density measurements of thin-film explosive material.

**Goal**: Non-destructive density measurements of thin-film.

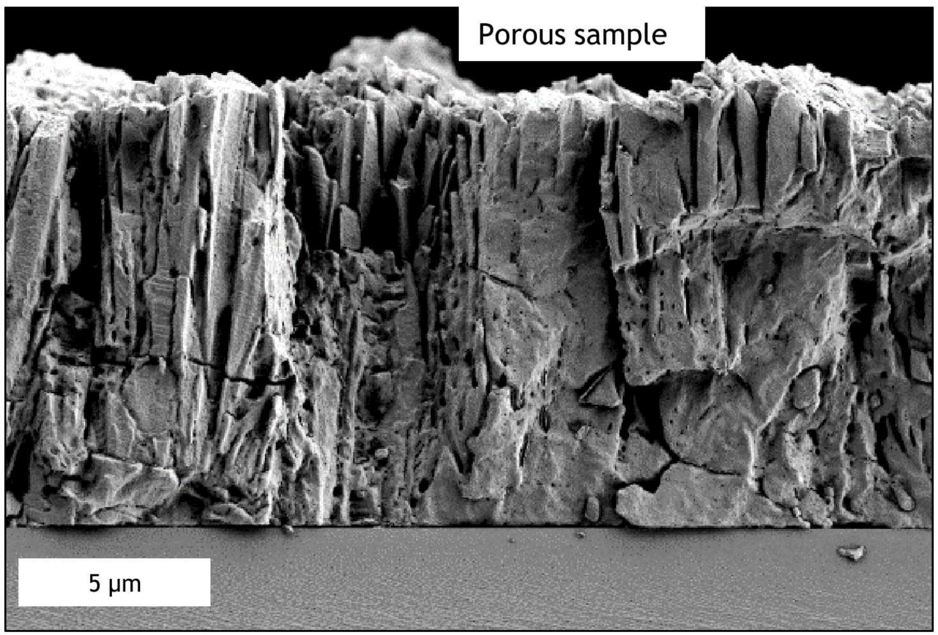


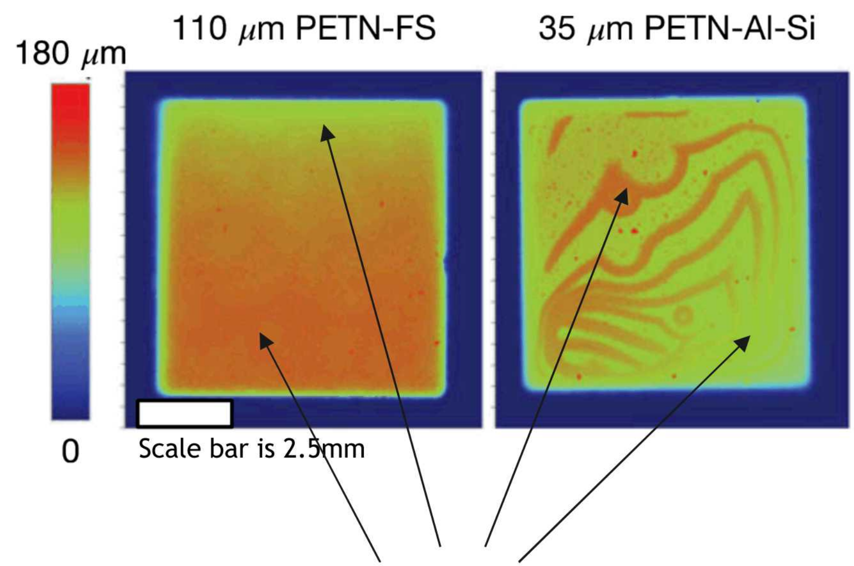


**Is the density uniform?**

<u>**Challenges**</u>:

- High uncertainty for thin-films
- Non-uniform growth

E. Ziade

# Traditional Density Measurements

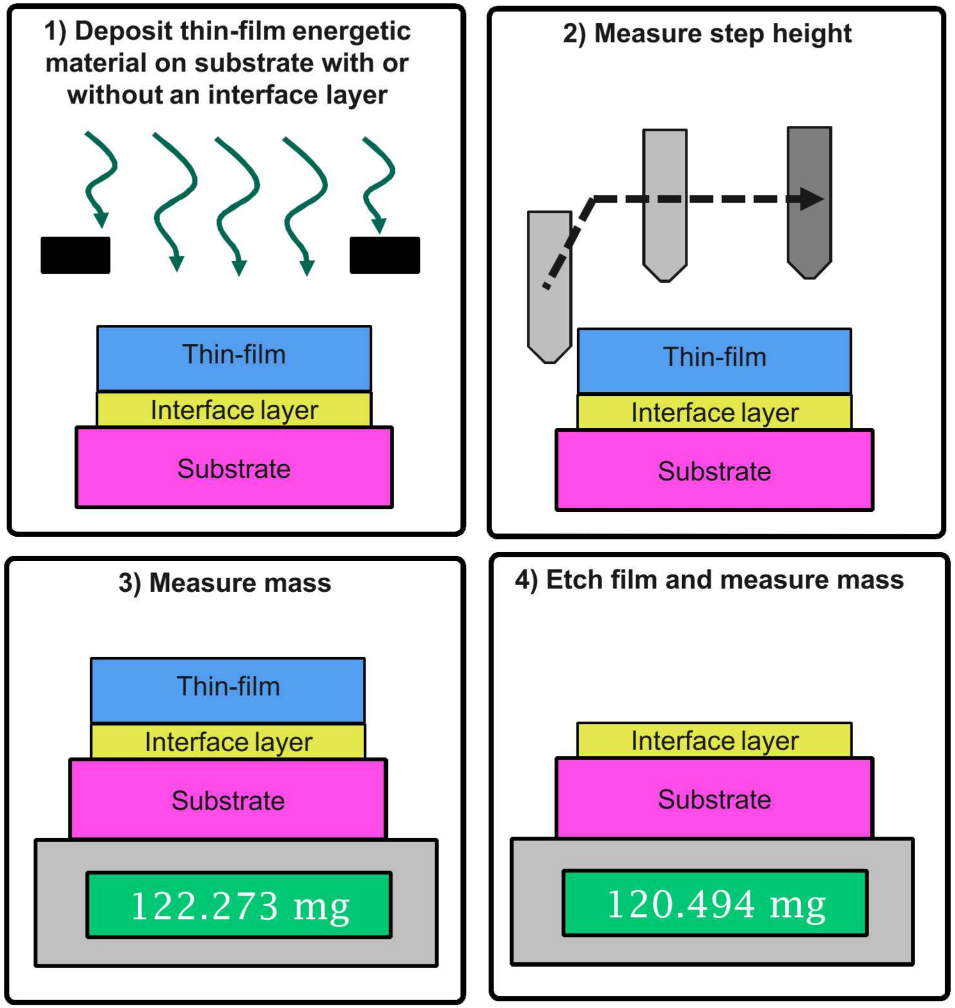


$$\rho = \frac{\Delta\text{mass}}{\text{Volume}}$$

**<u>Challenges</u>:**

- Need high accuracy scale
  - 100 µg error ~ 10% error in density

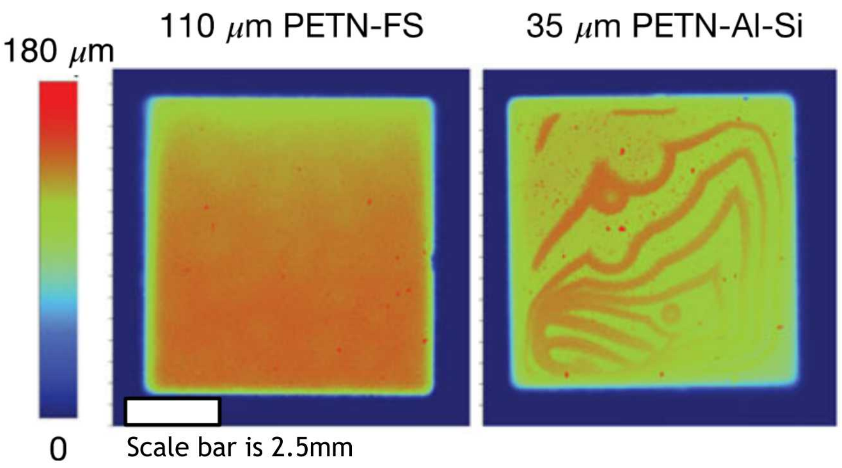


E. Ziade

# Thermal Waves for Density Measurements

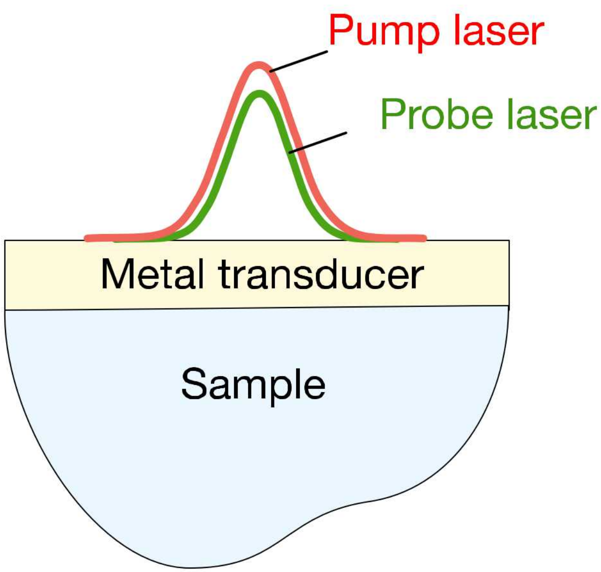


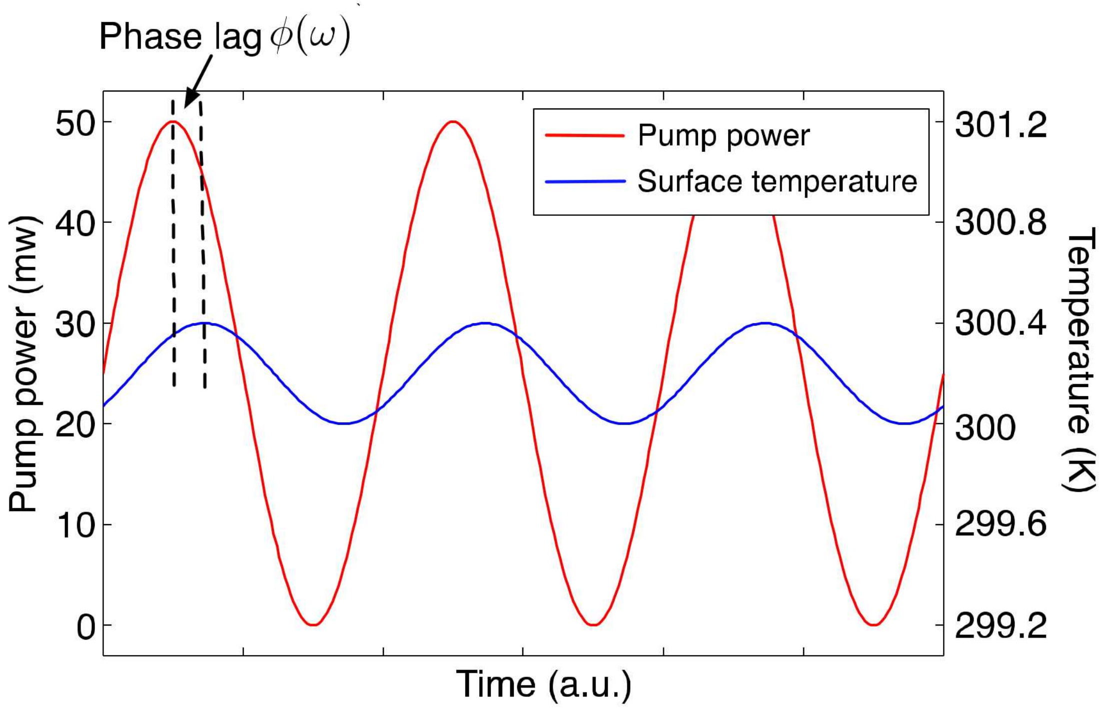


1) Periodic laser heats the sample (pump).
2) Surface temperature lags behind heat source because sample needs time to heat up.
3) Laser monitors surface temperature (probe).

[1] Schmidt, A. J., Cheaito, R., & Chiesa, M. (2009). A frequency-domain thermoreflectance method for the characterization of thermal properties. *The Review of Scientific Instruments*, *80*(9), 94901.
[2] Yang, J., **Ziade, E.** *et al*. (2014), Thermal conductance imaging of graphene contacts. *Journal of Applied Physics*, 116(2), 023515.
[3] **Ziade, E.,** *et al*. (2016), thickness dependent thermal conductivity of gallium nitride. *Applied Physics Letters,* 110(3), 031903.

# Thermal Waves for Density Measurements

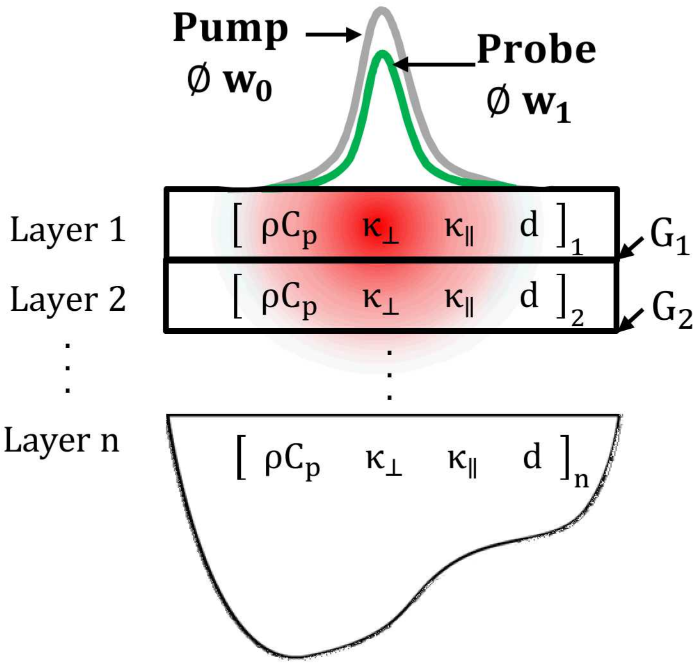


Parameters of interest

$$H(r,\omega) = \frac{\boxed{\kappa_{||}}}{r}\frac{\partial}{\partial r}\left(r\frac{\partial\theta}{\partial r}\right) + \boxed{\kappa_{\perp}}\frac{\partial^2\theta}{\partial z^2} = \boxed{C_p}\frac{\partial\theta}{\partial t}$$

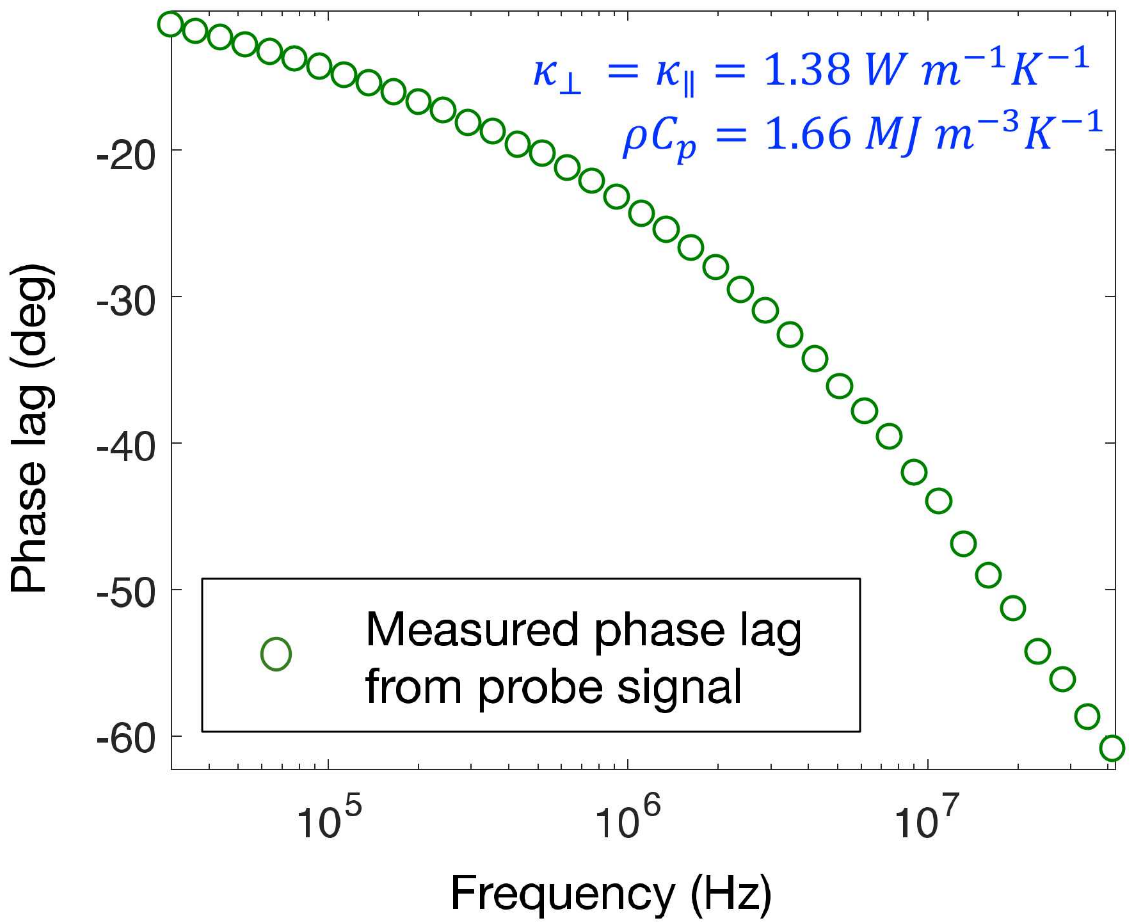


$\rho C_p$: Volumetric heat capacity

$\kappa_{\perp}$: Cross-plane thermal conductivity

$\kappa_{\parallel}$: In-plane thermal conductivity

d: Layer thickness

G: Thermal boundary conductance

E. Ziade

# Frequency Domain Thermoreflectance (FDTR)

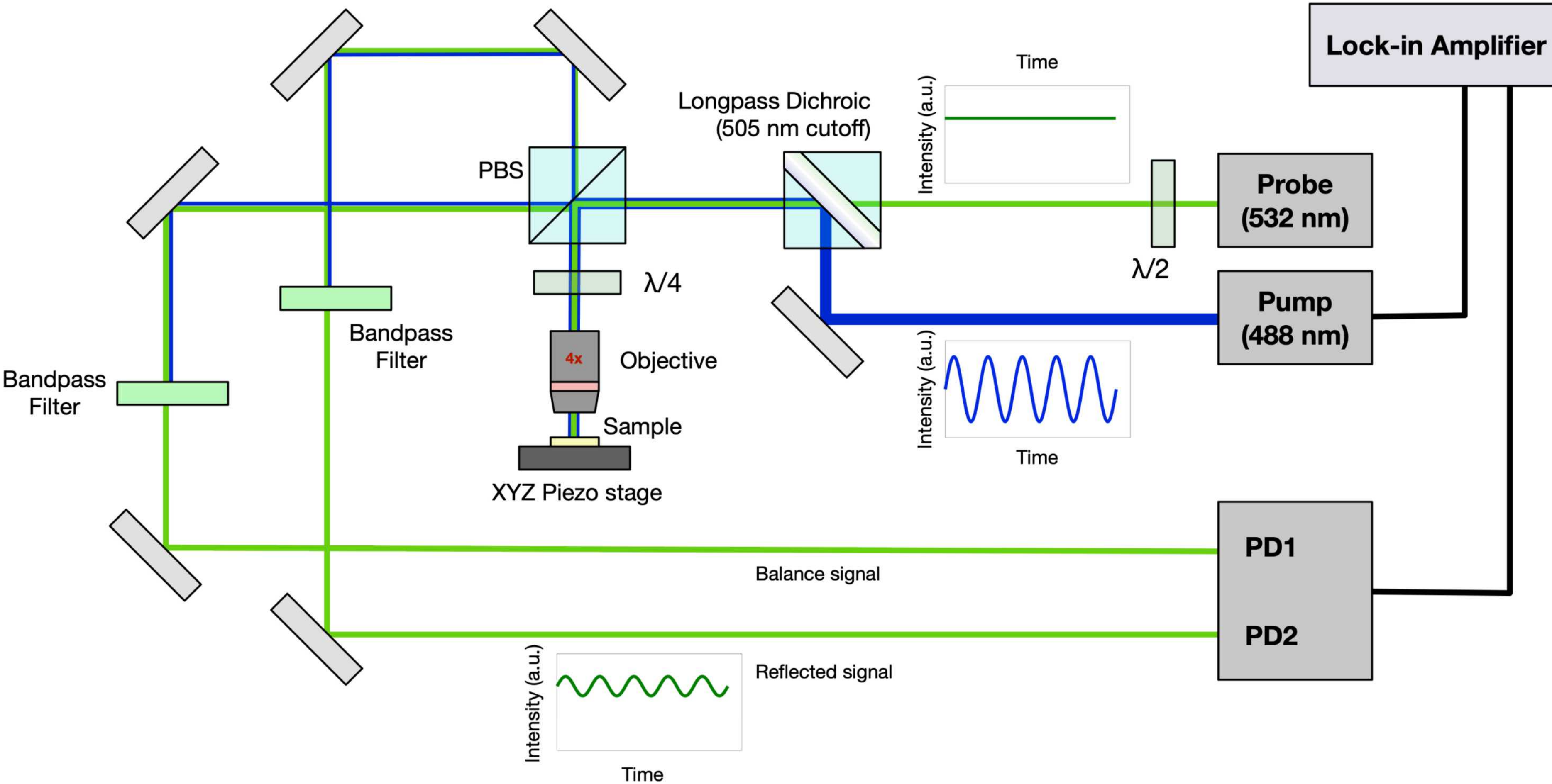


E. Ziade

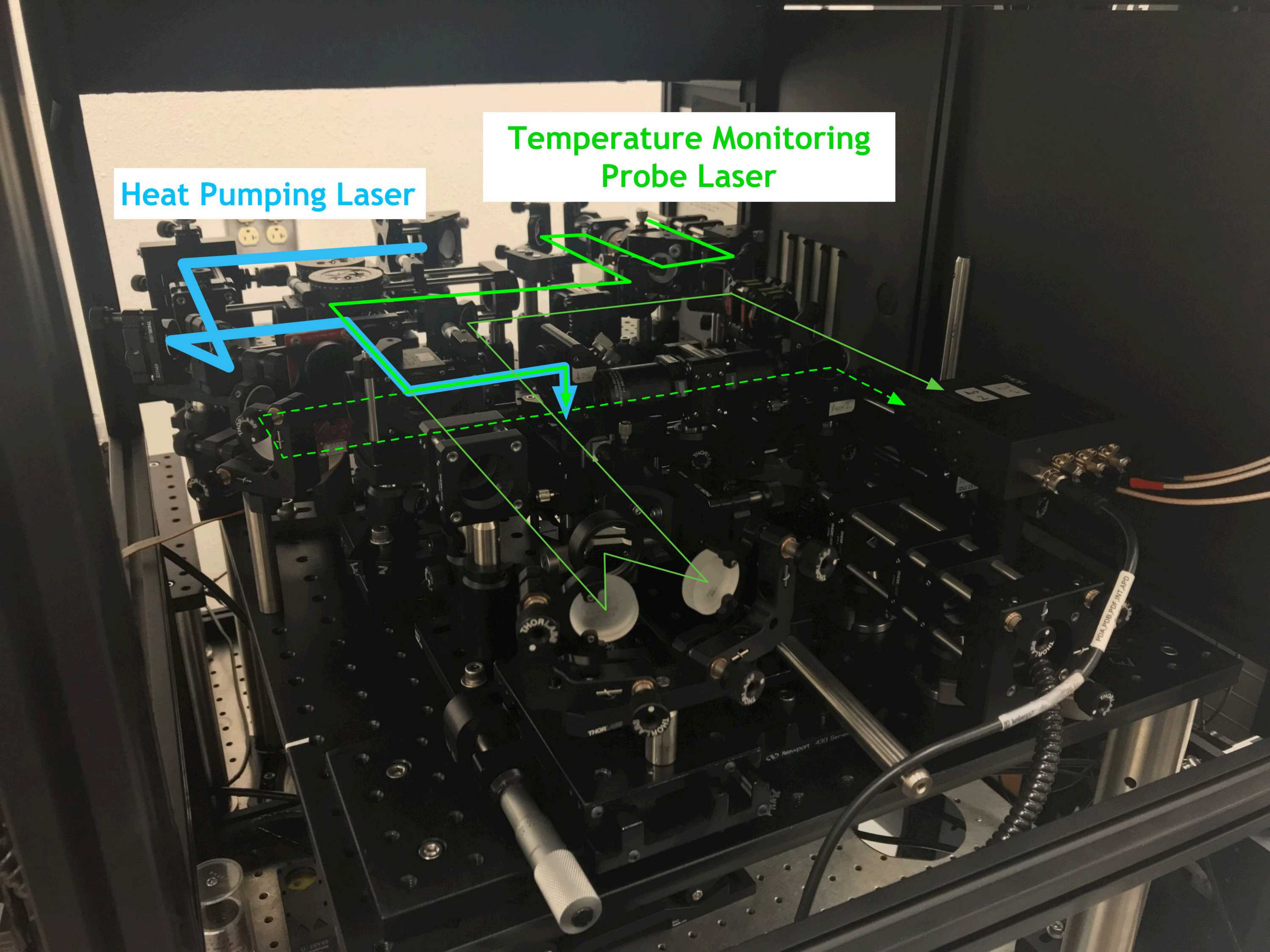
Heat Pumping Laser
Temperature Monitoring Probe Laser

# Samples

## 4 Indomethacin samples

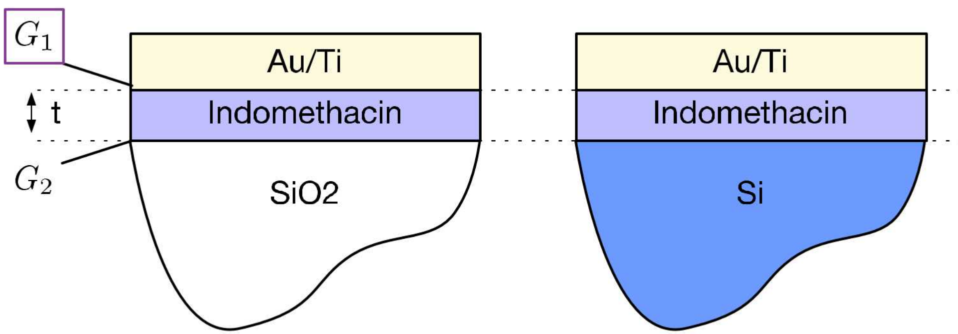


$$\begin{array}{l} [\;\rho C_p \quad \kappa_\perp \quad \kappa_{||} \quad d\;]_1 \\ [\;\boxed{\rho C_p} \quad \boxed{\kappa_\perp} \quad \kappa_{||} \quad t\;]_2 \\ [\;\rho C_p \quad \kappa_\perp \quad \kappa_{||} \quad d\;]_3 \end{array}$$

Nominal Thickness:
1 µm to 100 µm

## 5 PETN samples

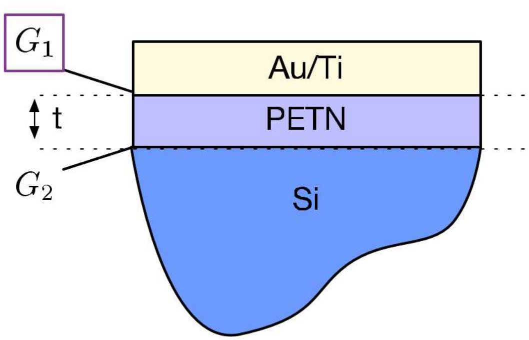


$$\begin{array}{l} [\;\rho C_p \quad \kappa_\perp \quad \kappa_{||} \quad d\;]_1 \\ [\;\boxed{\rho C_p} \quad \kappa_\perp \quad \kappa_{||} \quad t\;]_2 \\ [\;\rho C_p \quad \kappa_\perp \quad \kappa_{||} \quad d\;]_3 \end{array}$$

Nominal Thickness:
10 µm

# Thickness measurements – Indo-SiO2

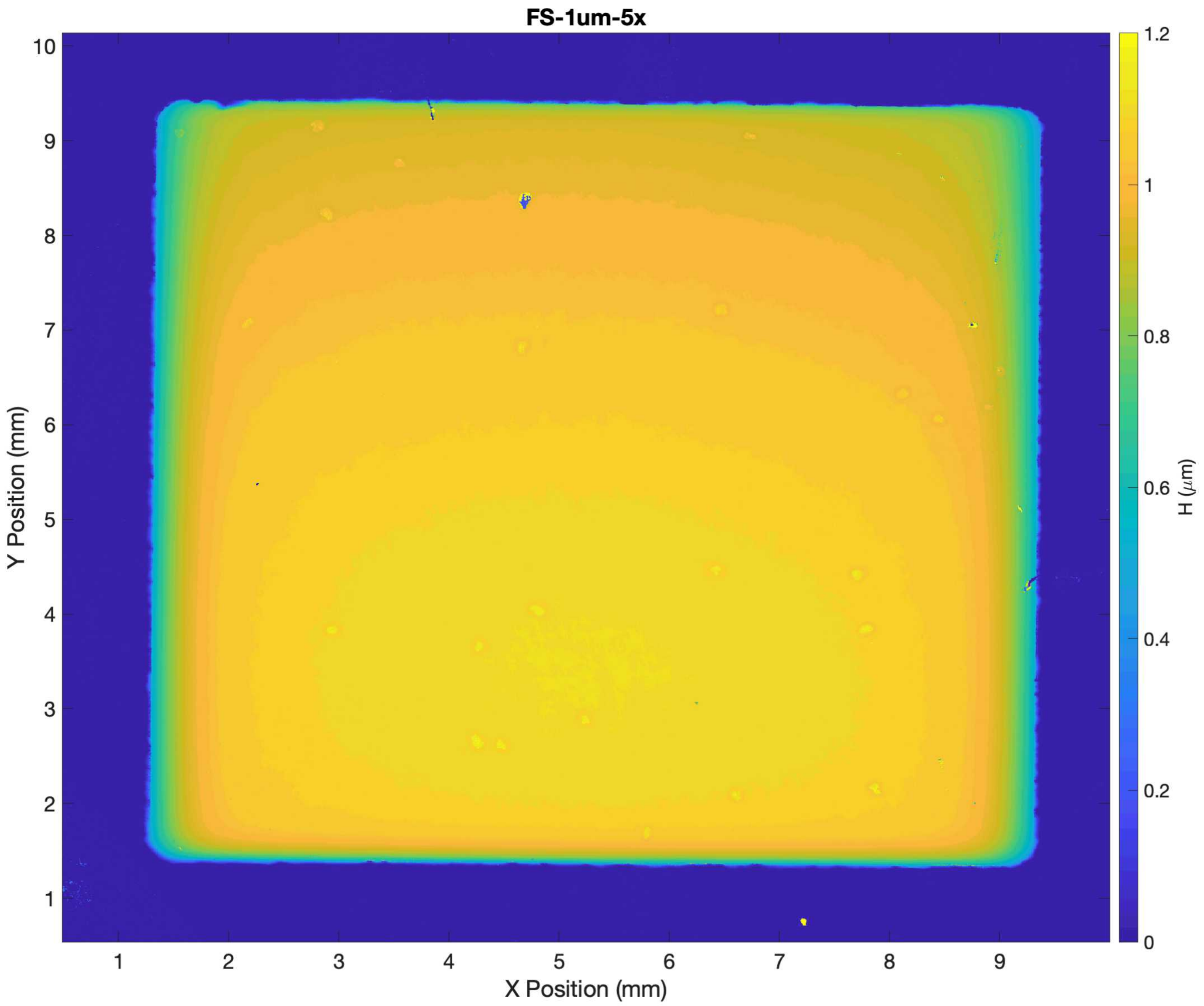


SiO2
Max – 1200 nm
Min – 890 nm

# Sensitivity Plots: Number of floated parameters

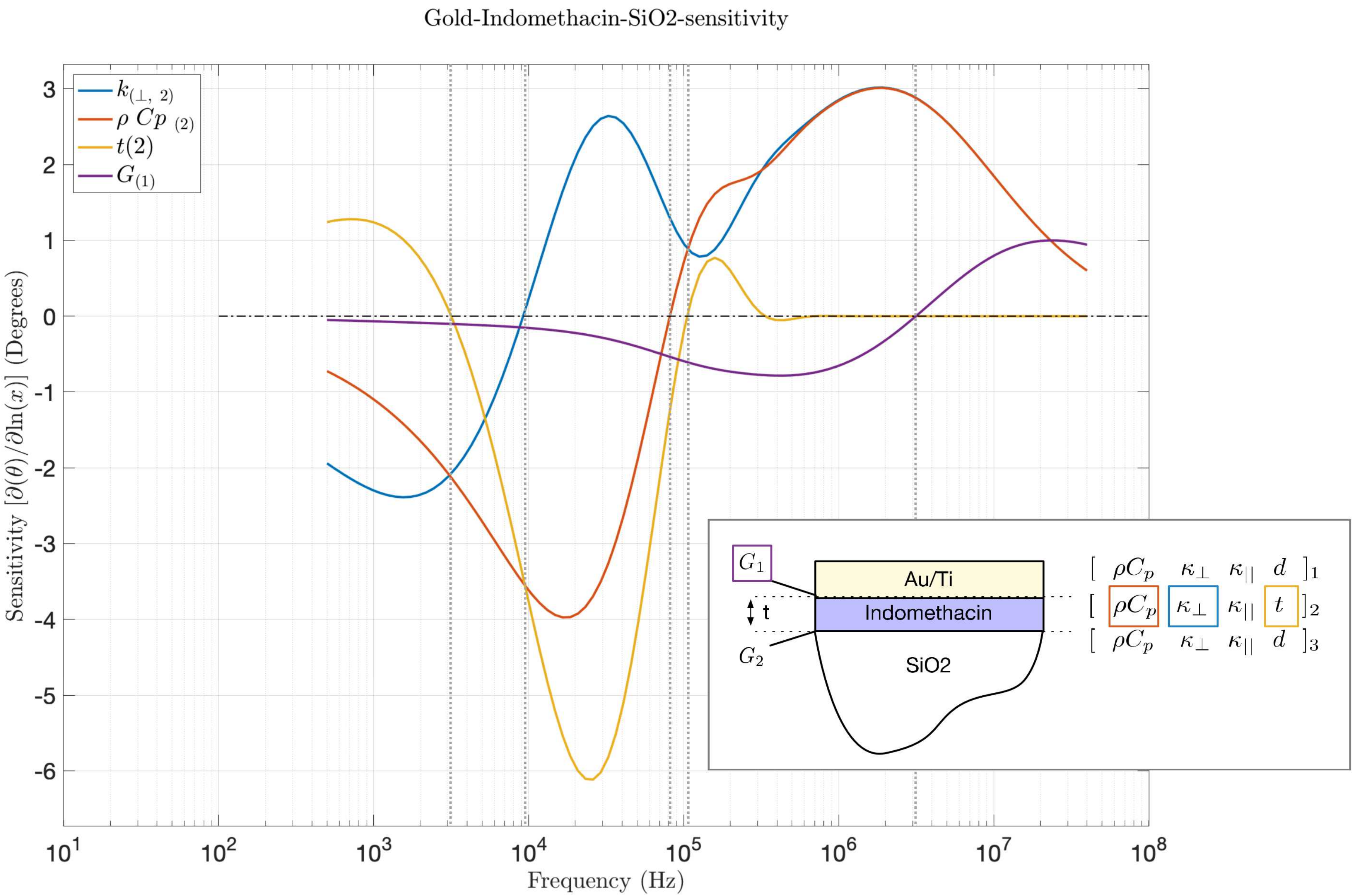

# FDTR Data Analysis

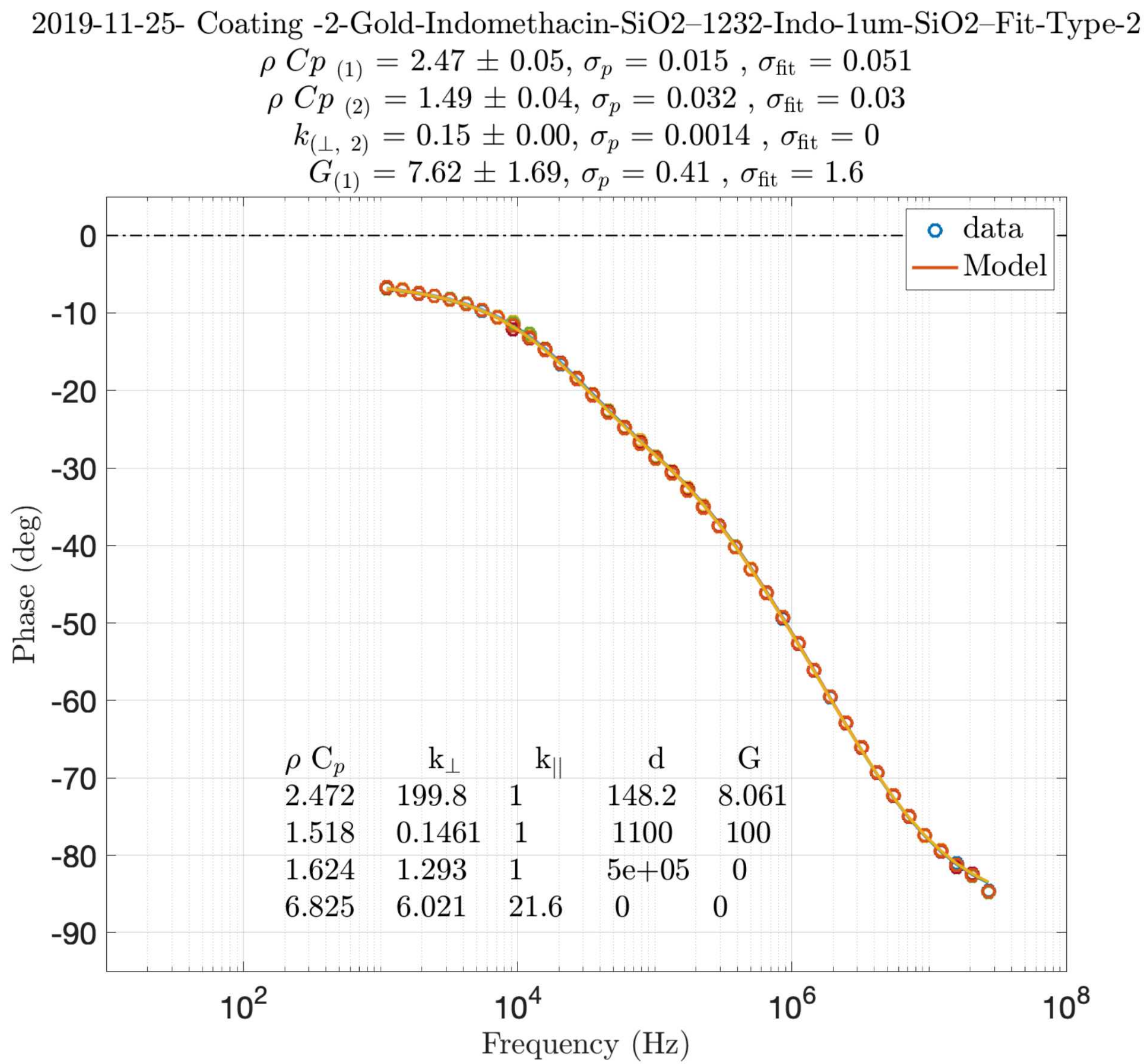

# Thickness measurements – Indo-Silicon

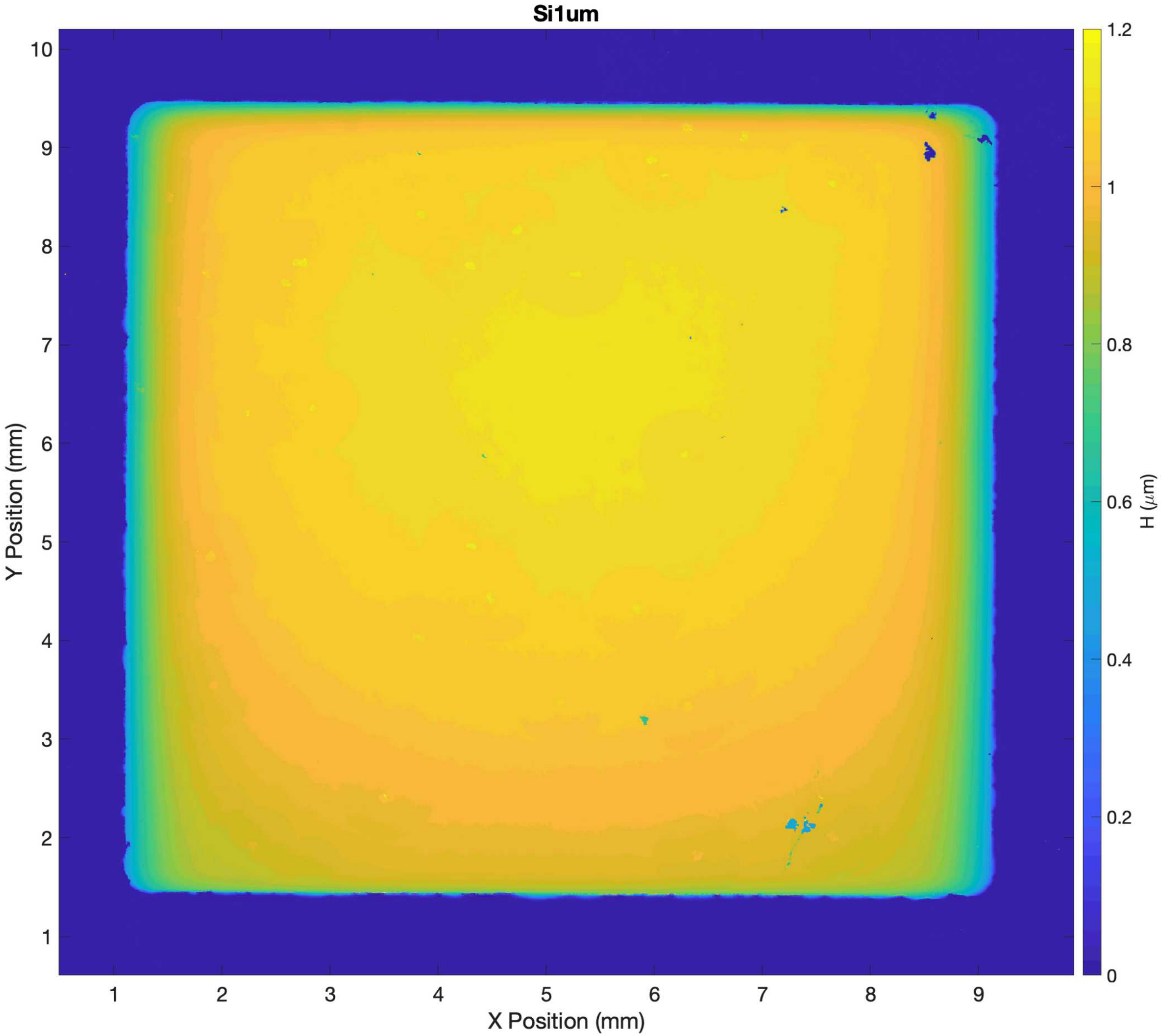


Si
Max – 1120 nm
Min – 830 nm

# Sensitivity Plots

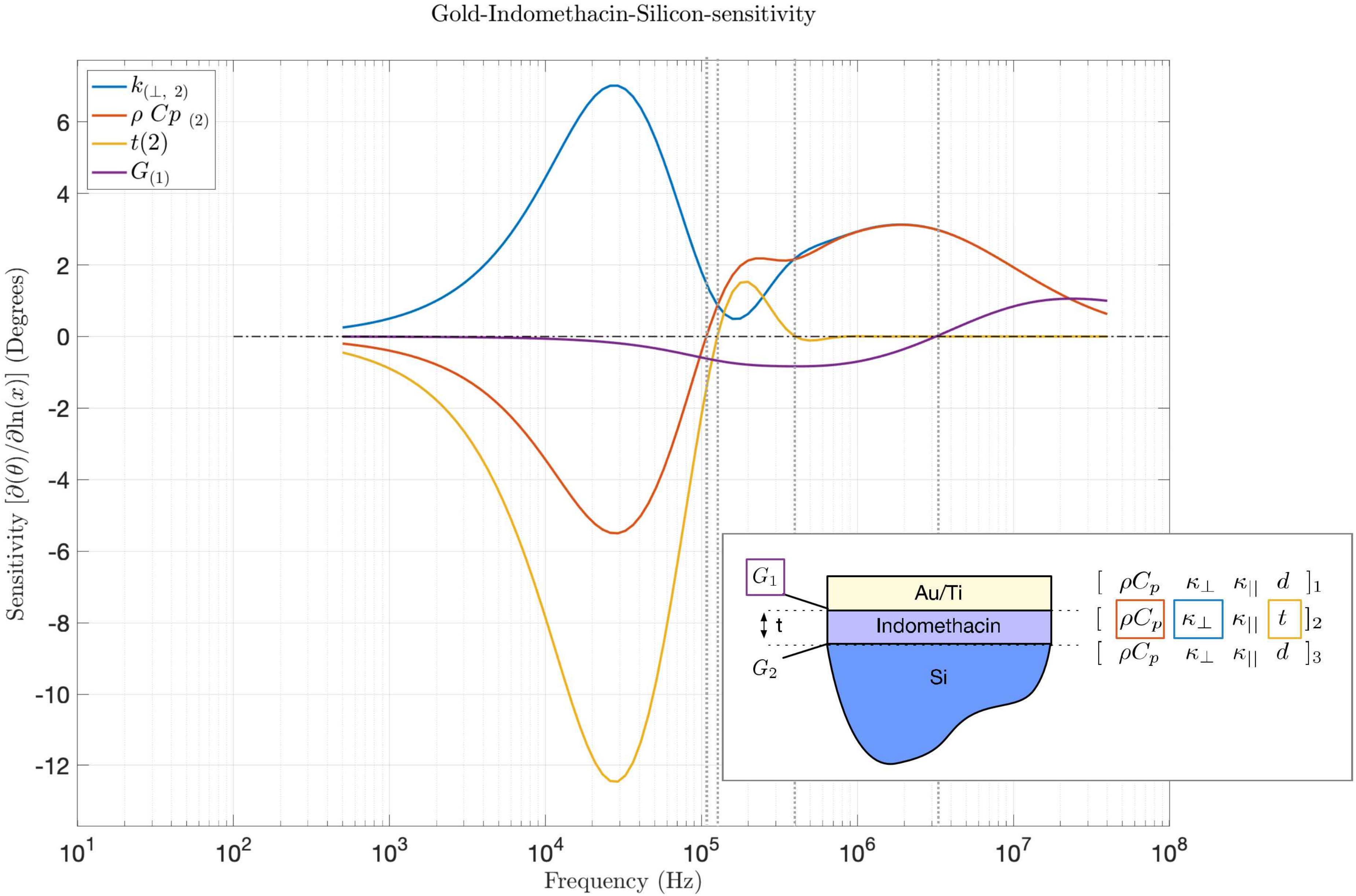

# FDTR Data Analysis

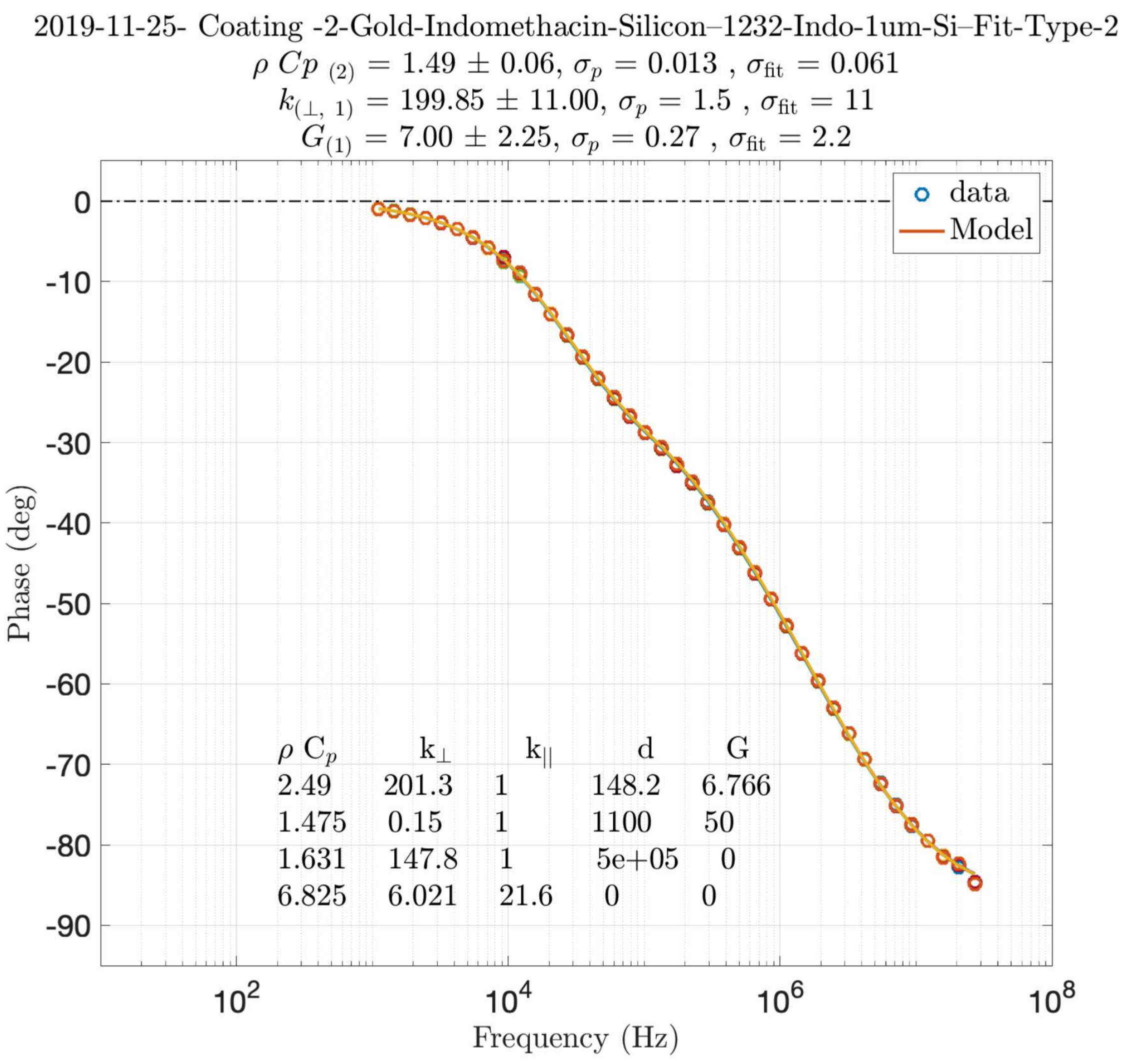

# Density Measurements of Encased Indomethacin

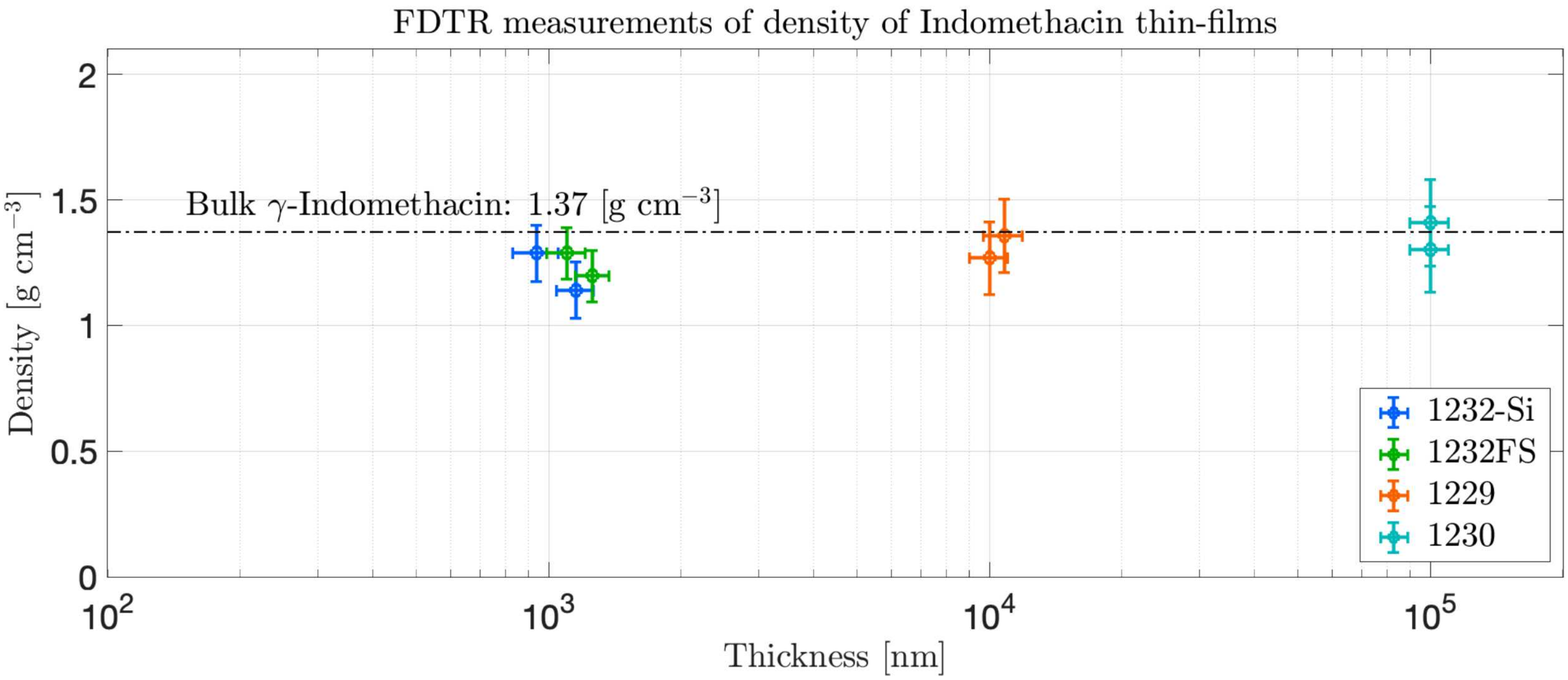


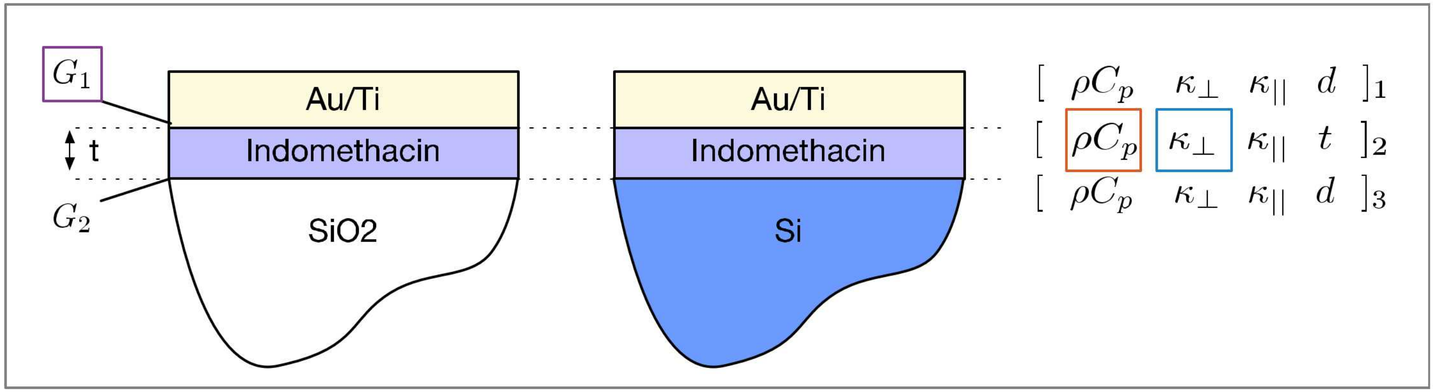

# Density Measurements of Encased PETN

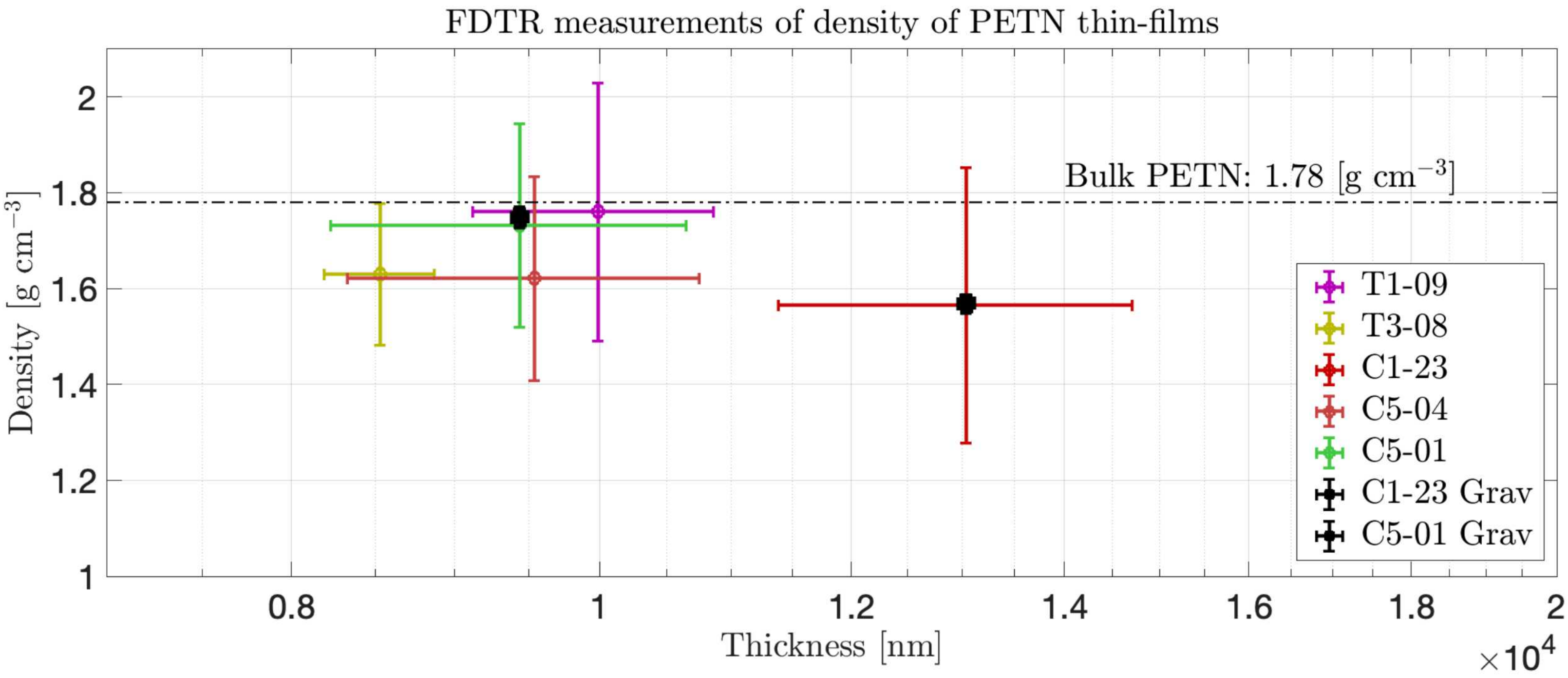


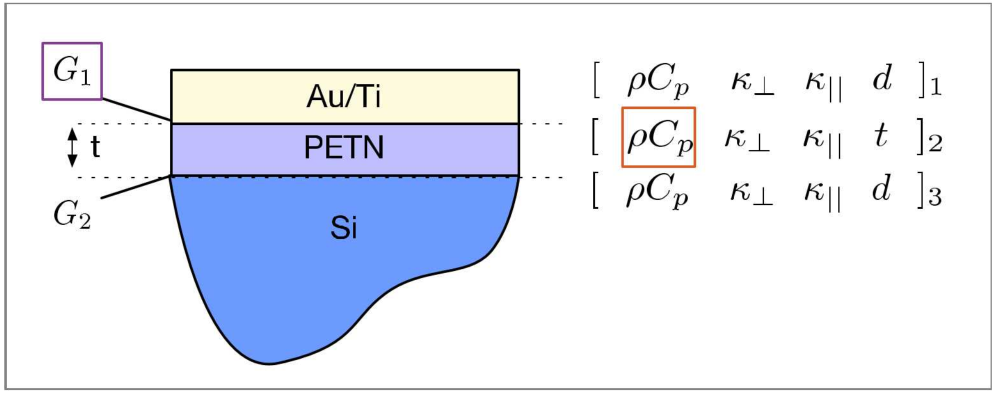

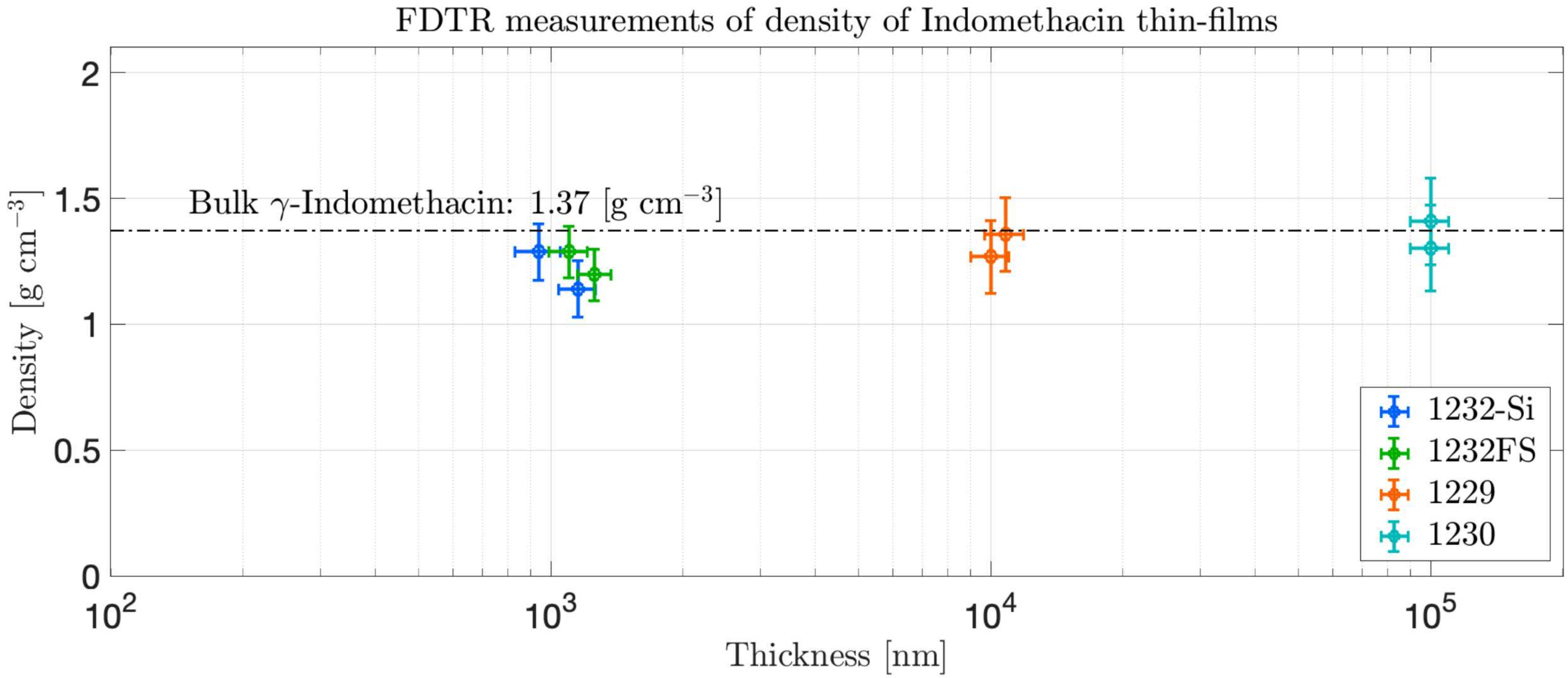
FDTR measurements of density of Indomethacin thin-films
Bulk γ-Indomethacin: 1.37 [g cm⁻³]
Density [g cm⁻³]
Thickness [nm]
1232-Si
1232FS
1229
1230


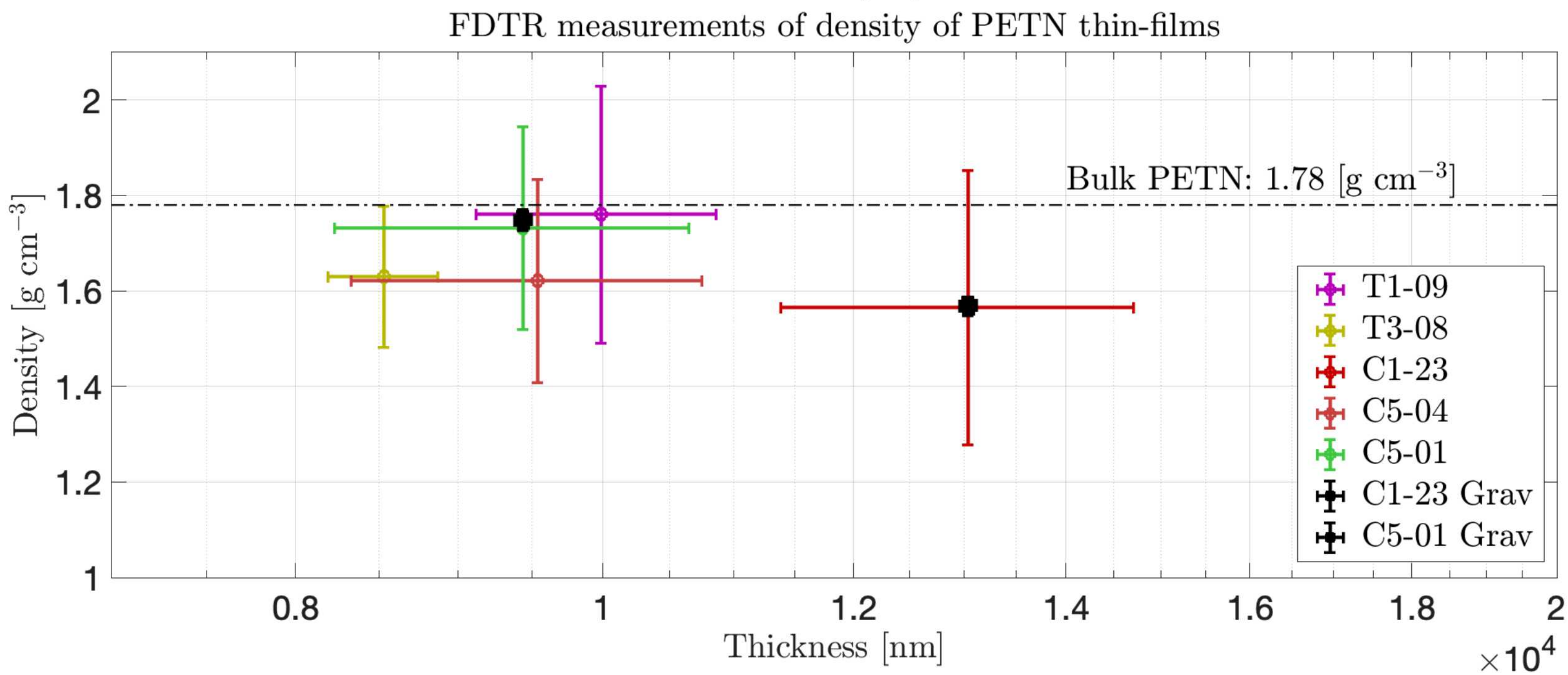
FDTR measurements of density of PETN thin-films
Bulk PETN: 1.78 [g cm⁻³]
Density [g cm⁻³]
Thickness [nm]
×10⁴
T1-09
T3-08
C1-23
C5-04
C5-01
C1-23 Grav
C5-01 Grav

# Thank you!

# Questions?

This work was supported in part, at the Center for Integrated Nanotechnologies, an Office of Science User Facility operated for the U.S. Department of Energy (DOE) Office of Science by Los Alamos National Laboratory (Contract DE-AC52-06NA25396) and Sandia National Laboratories (Contract DE-NA-0003525) and the Laboratory Directed Research and Development program at Sandia National Laboratories. Sandia National Laboratories is a multi-program laboratory managed and operated by National Technology and Engineering Solutions of Sandia, LLC., a wholly owned subsidiary of Honeywell International, Inc., for the U.S. Department of Energy's National Nuclear Security Administration under contract DE-NA-0003525.

# FDTR Data Analysis

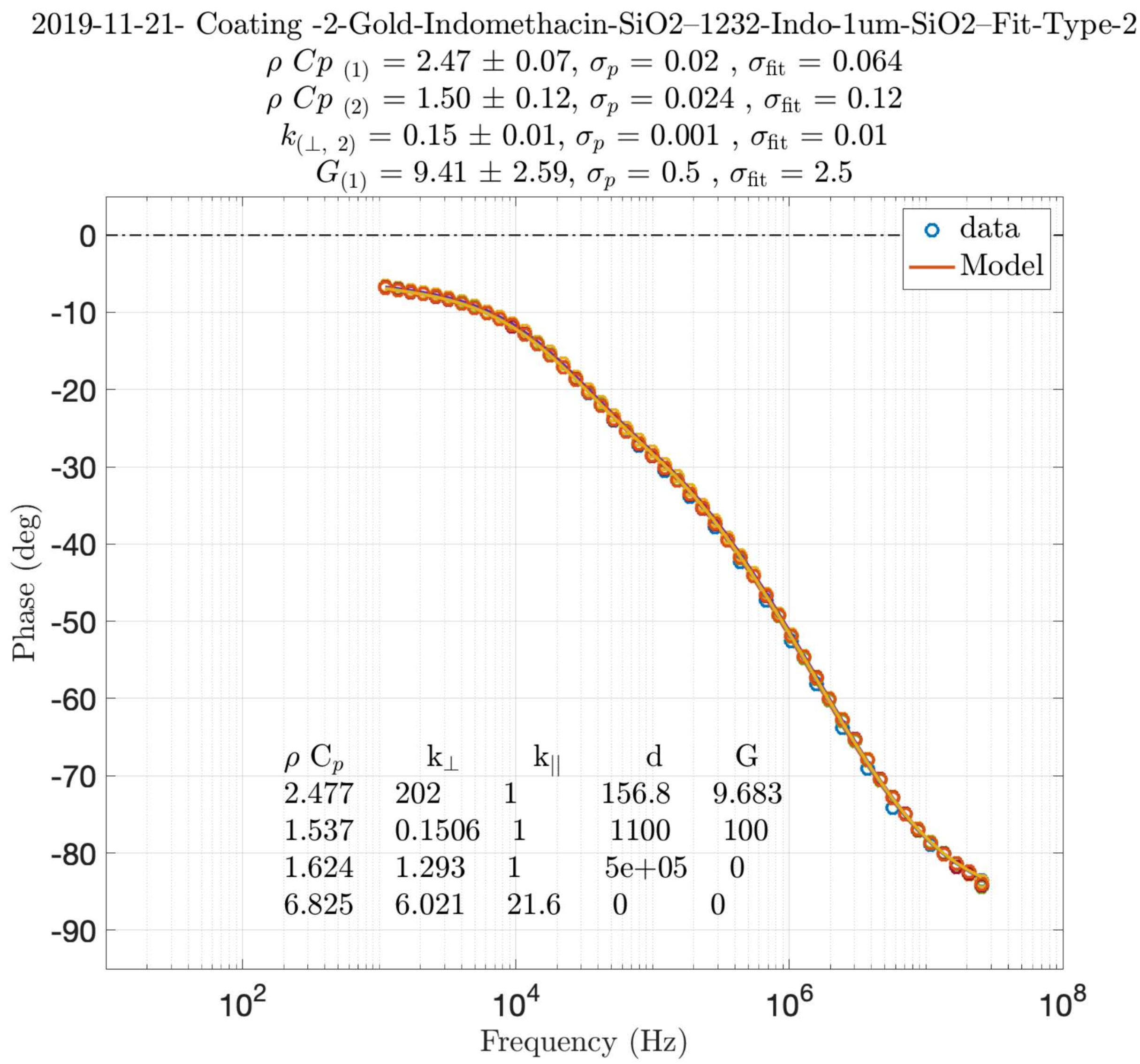

# FDTR Data Analysis

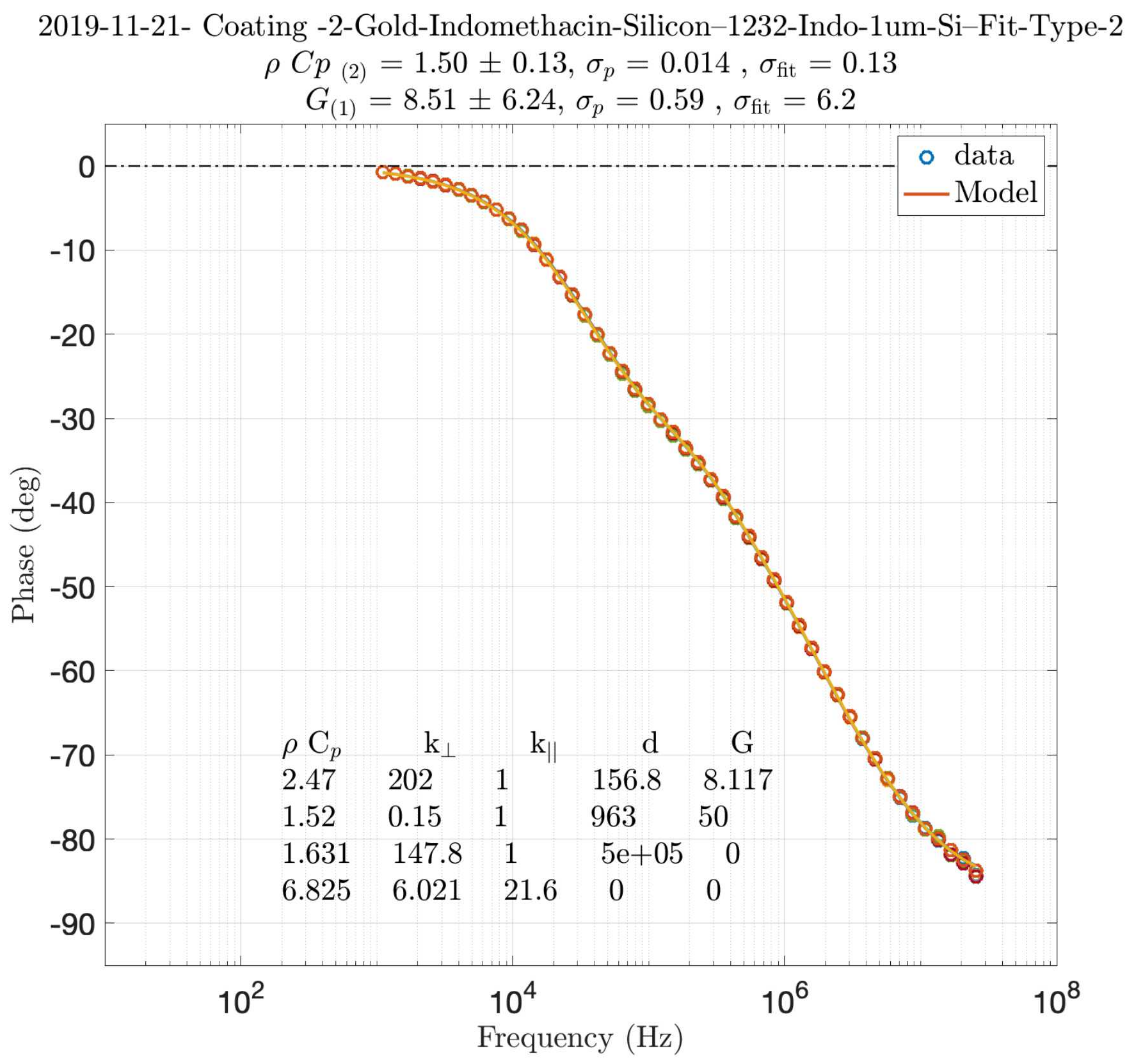

# FDTR Data Analysis

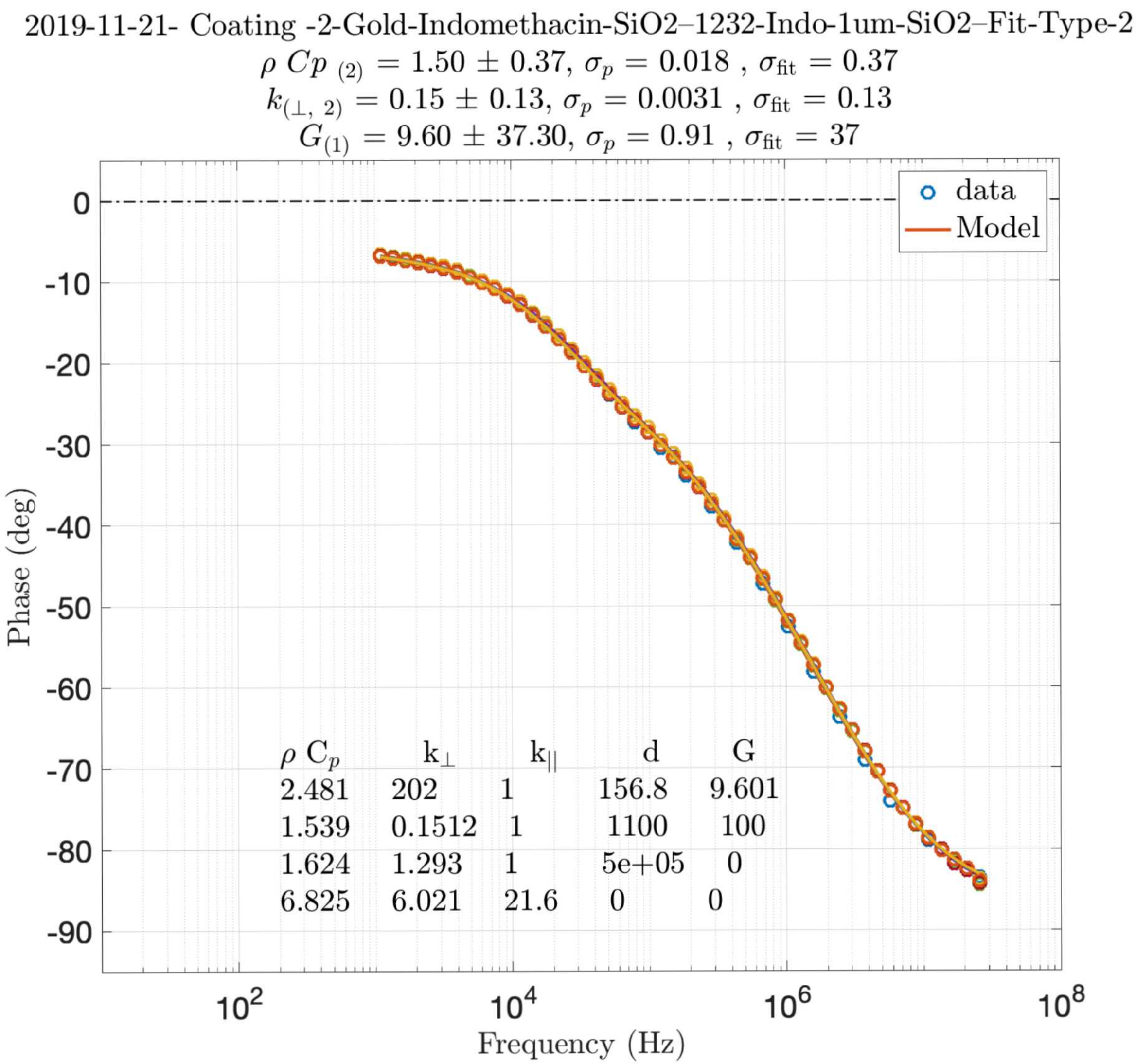

# Verification and Validation

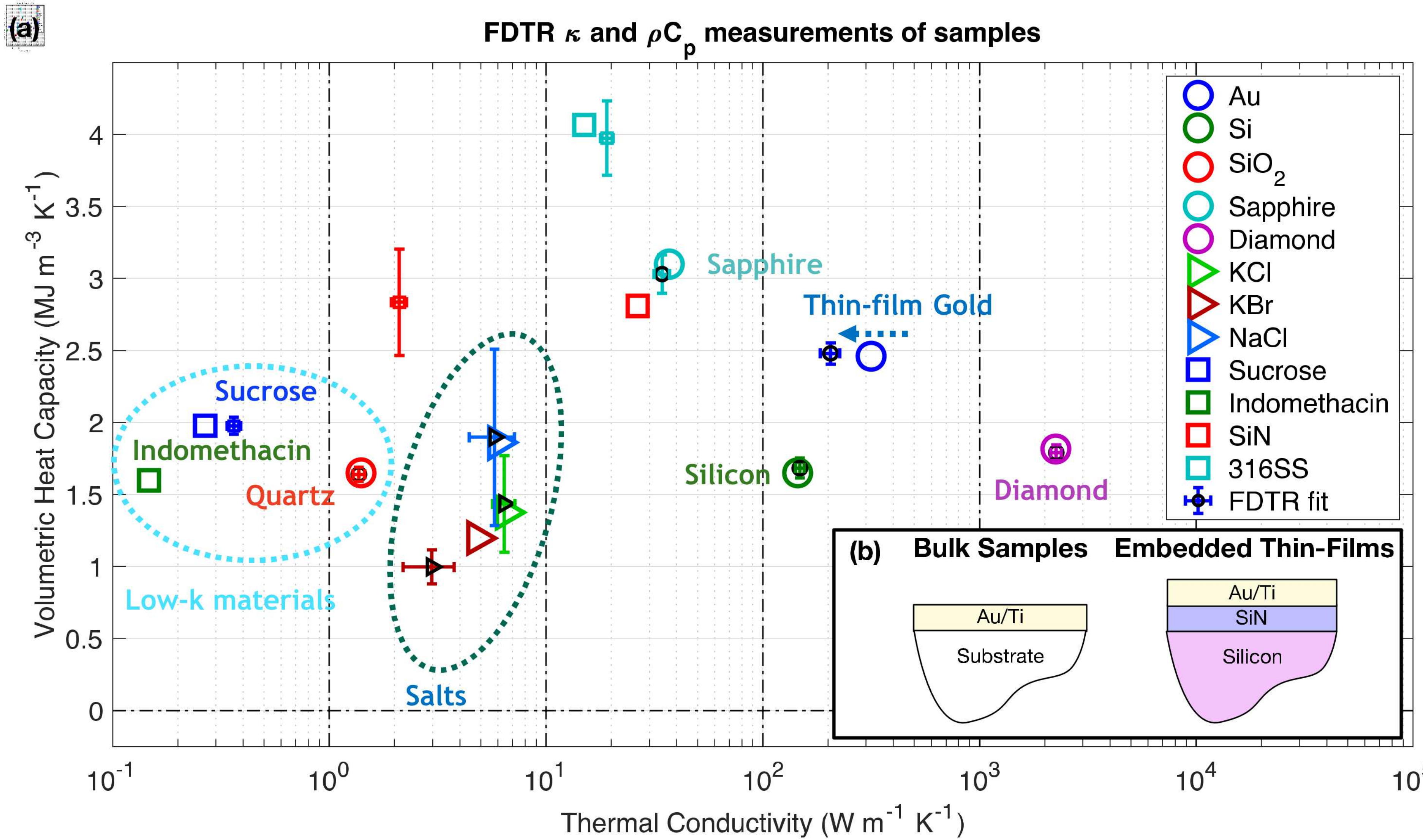


E. Ziade

# Verification and Validation

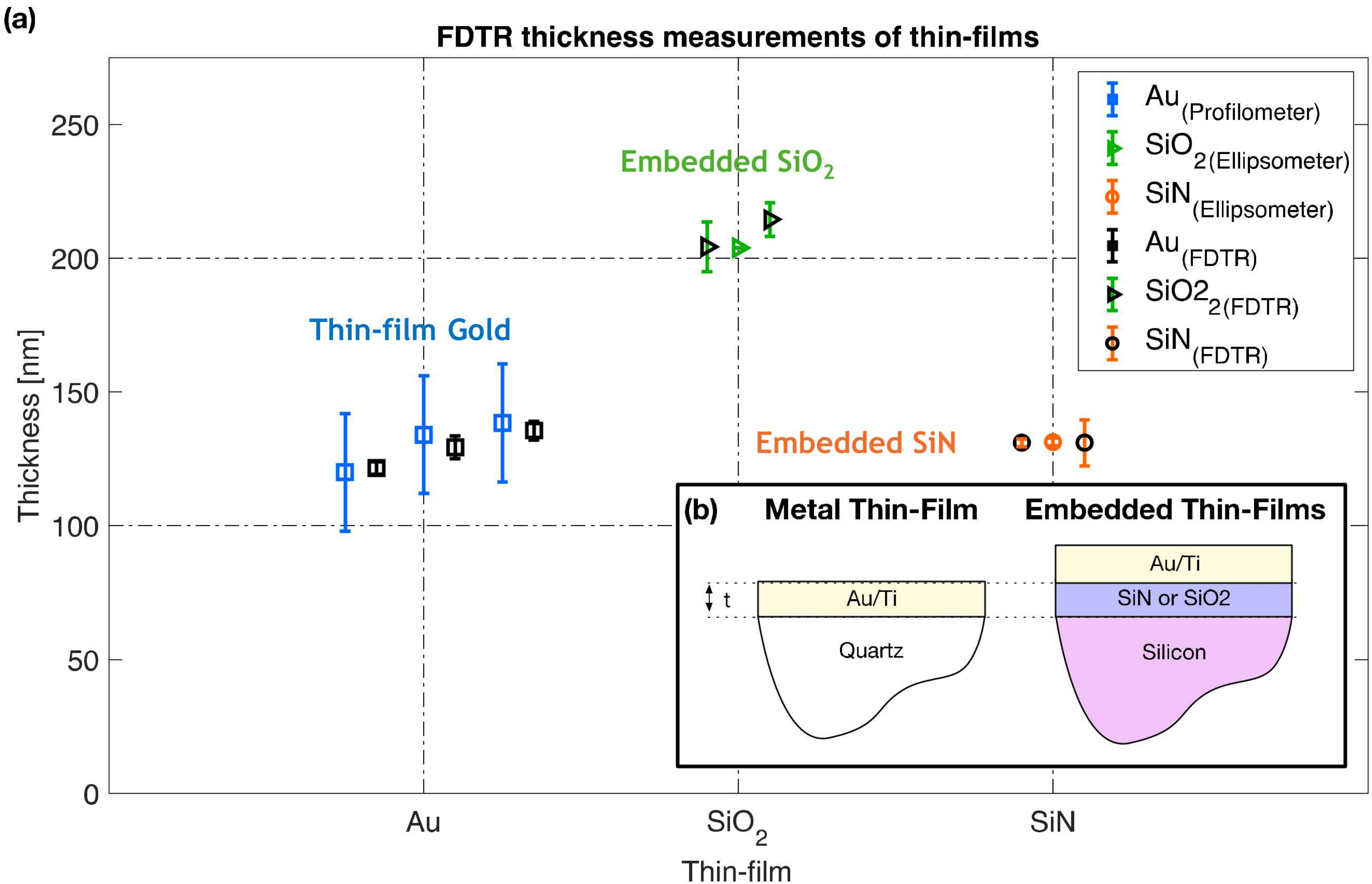

# Silicon

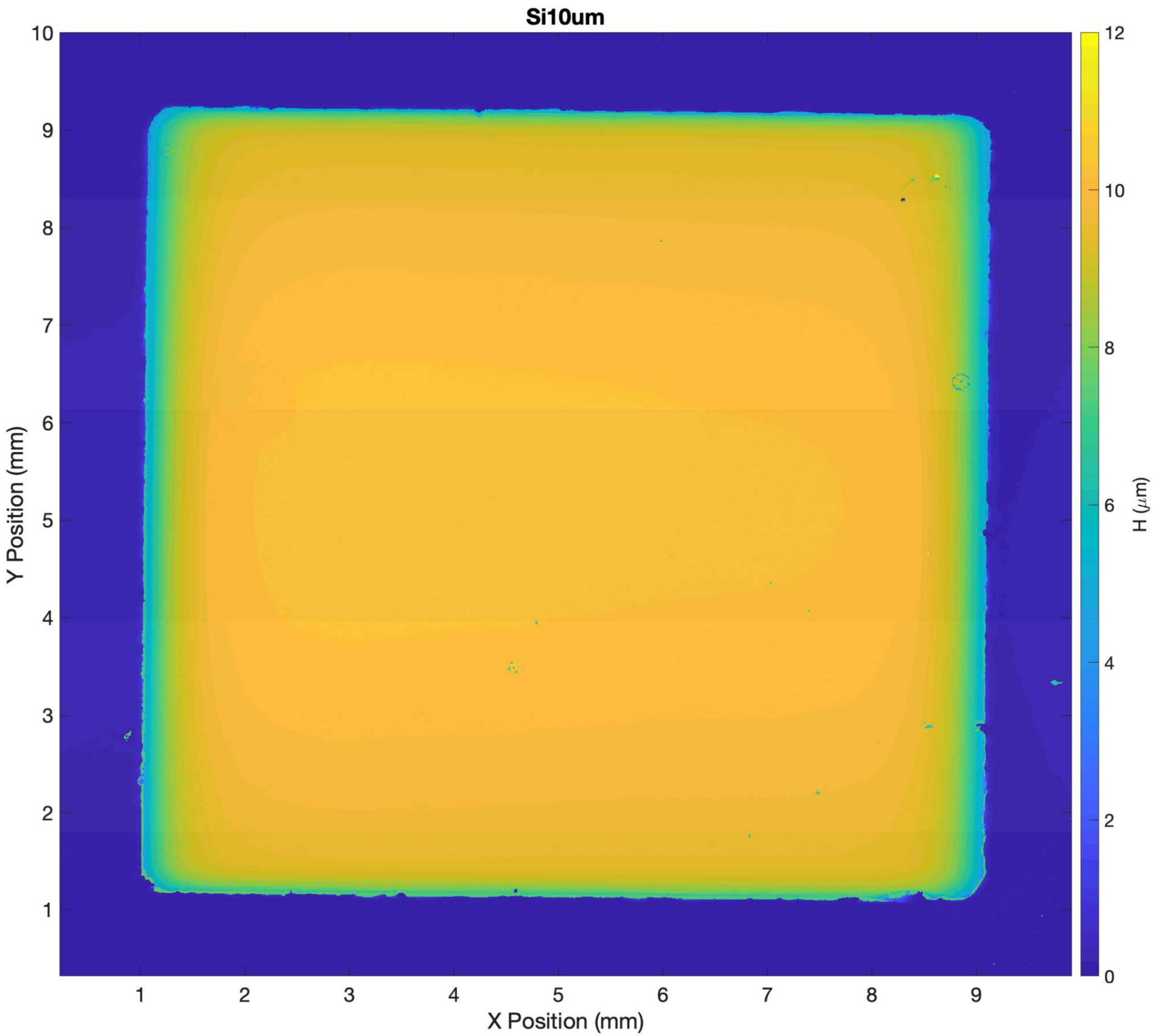

Si10um
10
9
8
7
6
5
4
3
2
1
Y Position (mm)
1
2
3
4
5
6
7
8
9
X Position (mm)
12
10
8
6
4
2
0
H ($\mu$m)

# FDTR Data Analysis

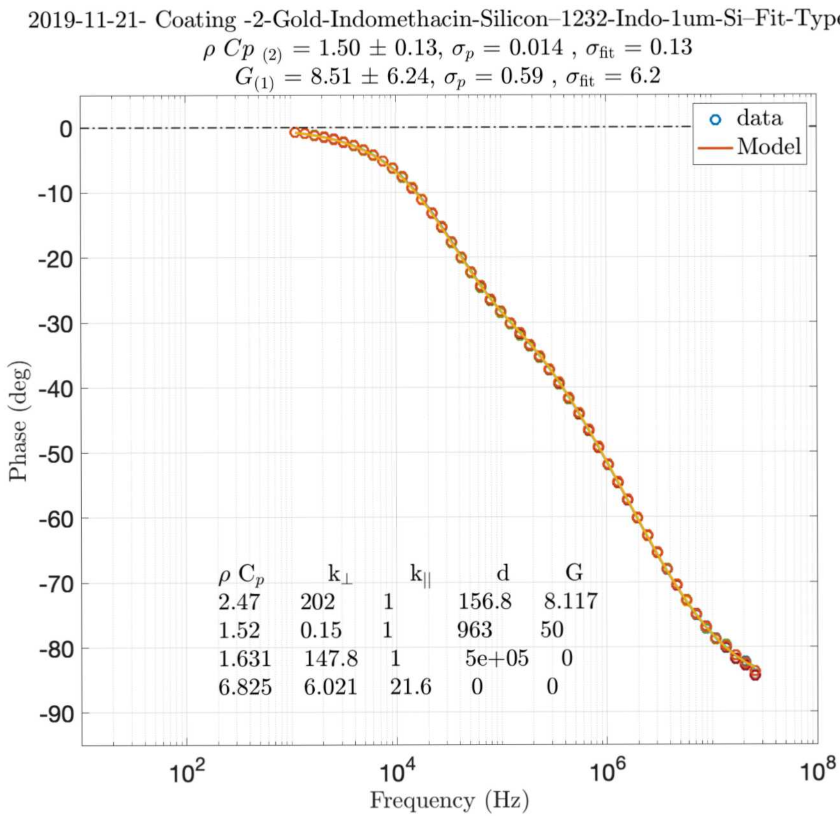


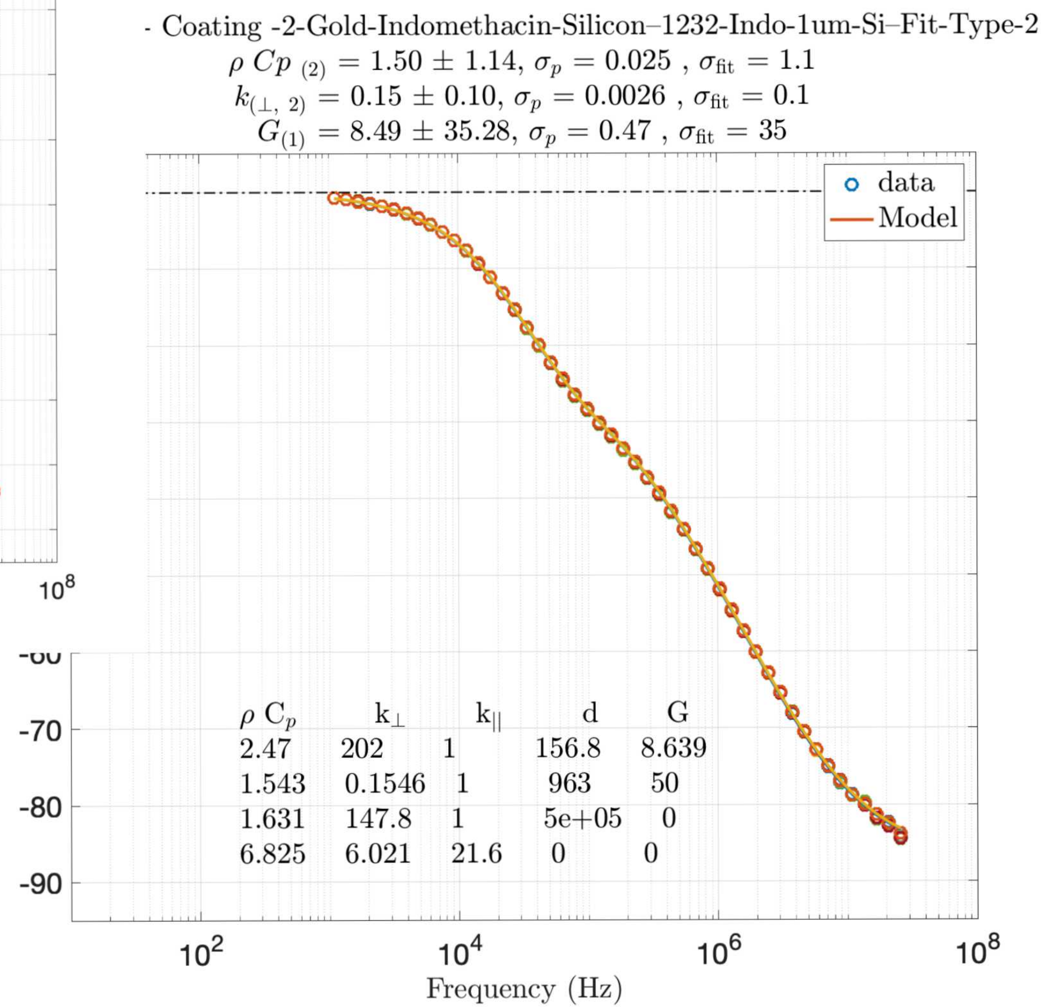

2019-10-15- Coating -2-Gold-Indomethacin-Silicon–1229-Indo-10um-Si–Fit-Type-2

$\rho\ Cp_{\ (2)} = 1.58 \pm 0.24,\ \sigma_p = 0.17\ ,\ \sigma_{\text{fit}} = 0.17$

$k_{(\perp,\ 2)} = 0.21 \pm 0.05,\ \sigma_p = 0.02\ ,\ \sigma_{\text{fit}} = 0.05$

$G_{(1)} = 6.66 \pm 0.61,\ \sigma_p = 0.45\ ,\ \sigma_{\text{fit}} = 0.4$

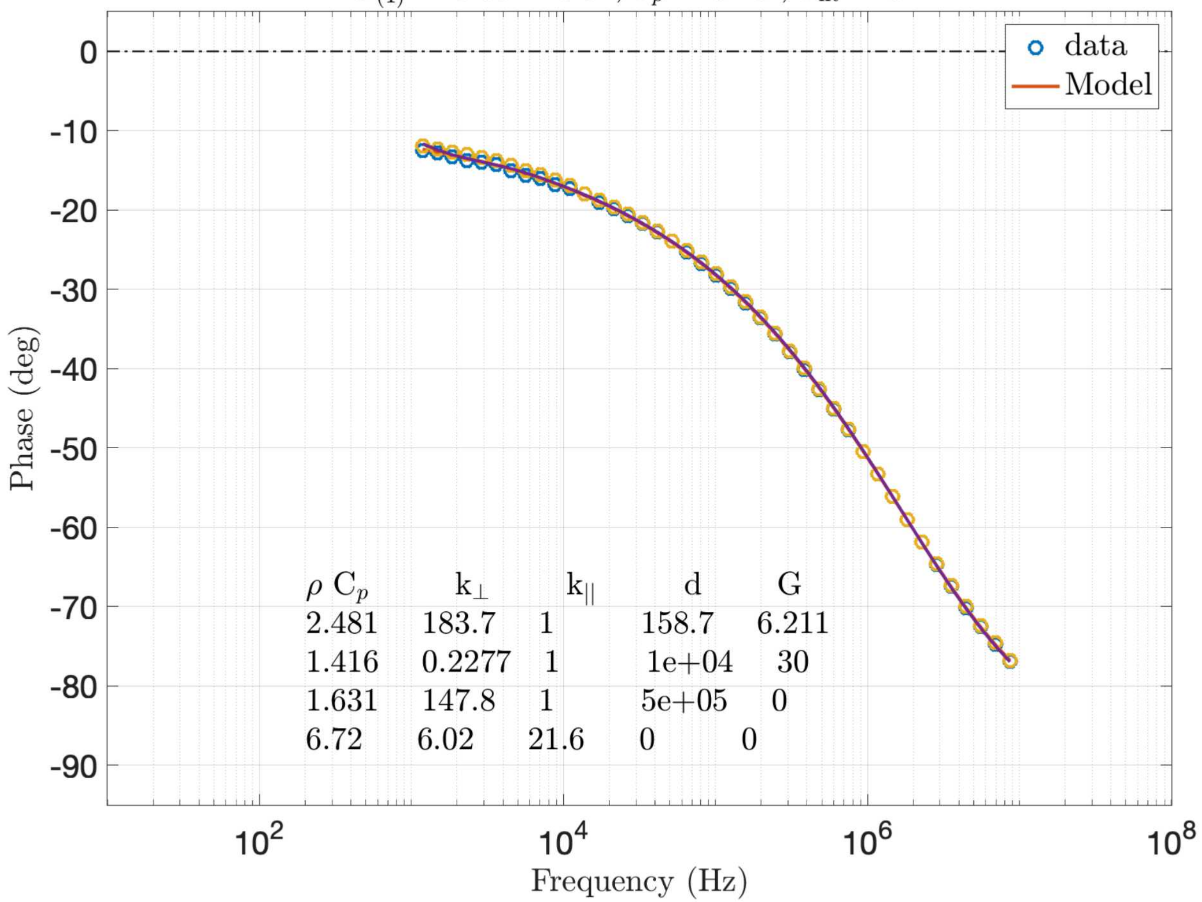


| | Thickness | | k cross 2 | | rhoCp | | Density | |
|---|---|---|---|---|---|---|---|---|
| | mean | std | mean | std | mean | std pop | mean | std |
| 1um SiO2 | 1040 | 55 | 0.16 | 0.02 | 1.52 | 0.038 | 1305 | ± 33 |
| 1um Si | 1080 | 170 | 0.18 | 0.048 | 1.55 | 0.011 | 1330 | ± 9 |
| 10um Si | | | 0.21 | 0.05 | 1.58 | 0.17 | 1356 | ± 146 |
| 100um Si | | | 0.18 | 0.04 | 1.64 | 0.076 | 1408 | ± 65 |

# Measurement

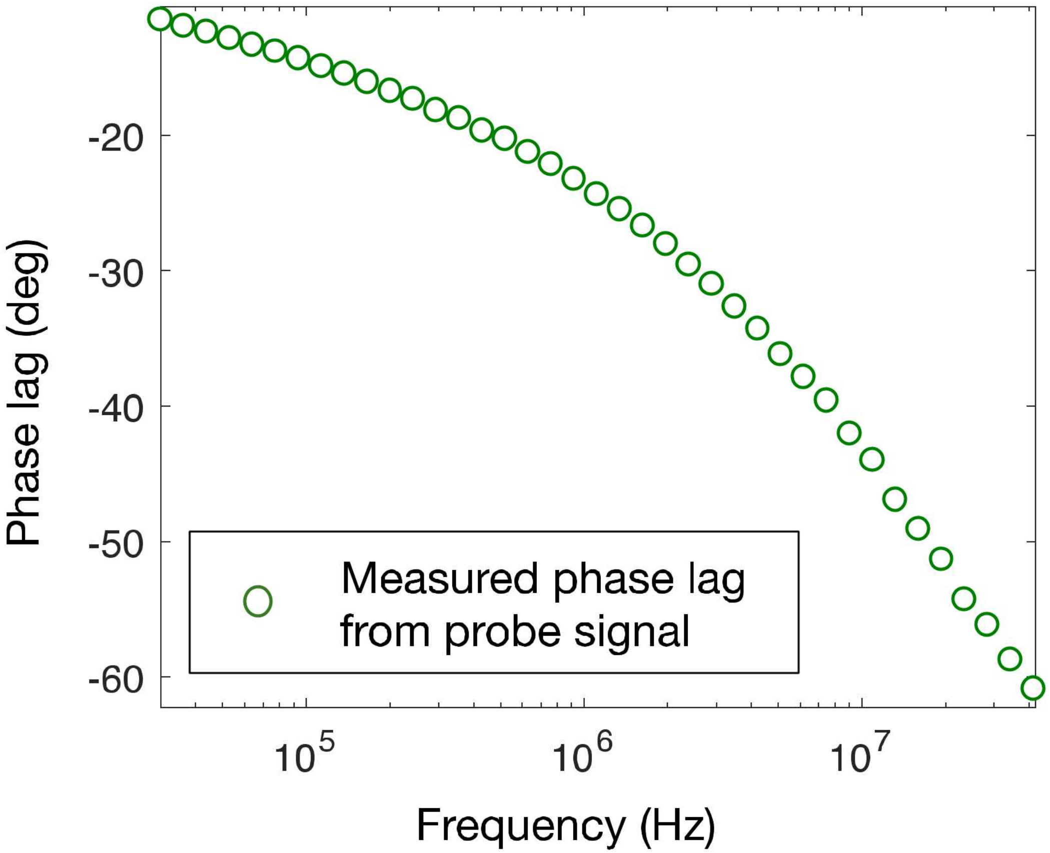


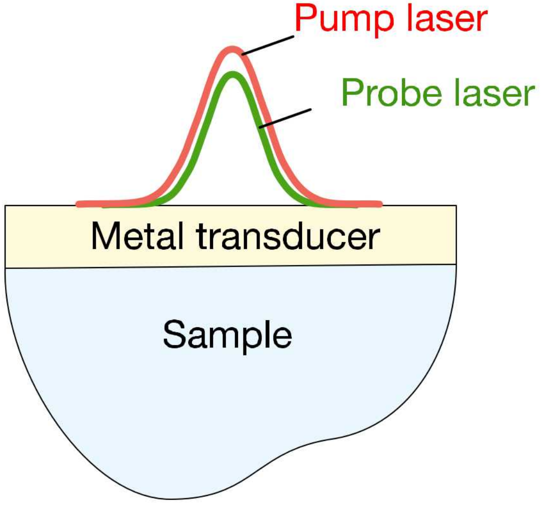


Measured phase lag

$$\underbrace{I_{\text{pump}}(r)e^{i\omega t}}_{\text{Periodic heat source}} \longrightarrow \underbrace{\boxed{H(r,\omega)}}_{\text{Thermal model}} \longrightarrow \underbrace{T(r,\omega)e^{i[\omega t+\boxed{\phi(r,w)]}}}_{\text{Surface temperature}}$$

Variance-Covariance Matrix

$$\boxed{\mathrm{Var}[\boldsymbol{b_u}]} = E[\boldsymbol{b_u}^2] = \boxed{(\boldsymbol{J_u^*}'\boldsymbol{J_u^*})^{-1}}\ \boldsymbol{J_u^*}'\ [\boxed{\mathrm{Var}[\boldsymbol{y}]} + \boxed{\boldsymbol{J_c^*}\ \mathrm{Var}[\boldsymbol{b_c}]\ \boldsymbol{J_c^*}'}]\ \boldsymbol{J_u^*}(\boldsymbol{J_u^*}'\boldsymbol{J_u^*})^{-1}$$

Error in model (residuals)

$$\sigma_y^2 = s_y^2 = \frac{\boldsymbol{e}'\boldsymbol{e}}{n-k}$$

$$E[\boldsymbol{e}'\boldsymbol{e}] = E[\mathrm{tr}(\boldsymbol{e}'\boldsymbol{e})] = s_y^2(n-k)$$

Uncertainty in controlled parameters

$$\boldsymbol{J_u^*} = \begin{bmatrix} \frac{\partial f(x_1,\mathbf{b})}{\partial b_1}\Big|_{\boldsymbol{b}*} & \cdots & \frac{\partial f(x_1,\mathbf{b})}{\partial b_p}\Big|_{\boldsymbol{b}*} \\ \vdots & \ddots & \vdots \\ \frac{\partial f(x_n,\mathbf{b})}{\partial b_1}\Big|_{\boldsymbol{b}*} & \cdots & \frac{\partial f(x_n,\mathbf{b})}{\partial b_p}\Big|_{\boldsymbol{b}*} \end{bmatrix} \qquad \boldsymbol{J_c^*} = \begin{bmatrix} \frac{\partial f(x_1,\mathbf{b})}{\partial b_{p+1}}\Big|_{\boldsymbol{b}*} & \cdots & \frac{\partial f(x_1,\mathbf{b})}{\partial b_P}\Big|_{\boldsymbol{b}*} \\ \vdots & \ddots & \vdots \\ \frac{\partial f(x_n,\mathbf{b})}{\partial b_{p+1}}\Big|_{\boldsymbol{b}*} & \cdots & \frac{\partial f(x_n,\mathbf{b})}{\partial b_P}\Big|_{\boldsymbol{b}*} \end{bmatrix}$$

$$\mathrm{Var}[\boldsymbol{y}] = \begin{bmatrix} \sigma_{y_1}^2 & 0 & 0 & \cdots \\ 0 & \sigma_{y_2}^2 & 0 & \cdots \\ 0 & 0 & \sigma_{y_3}^2 & \cdots \\ \vdots & \vdots & \vdots & \ddots \end{bmatrix}$$

$$\mathrm{Var}[\boldsymbol{b_u}] = \begin{bmatrix} \sigma_{b_1}^2 & \mathrm{cov}[b_1,b_2] & \mathrm{cov}[b_1,b_3] & \cdots \\ \mathrm{cov}[b_2,b_1] & \sigma_{b_2}^2 & \mathrm{cov}[b_2,b_3] & \cdots \\ \mathrm{cov}[b_3,b_1] & \mathrm{cov}[b_3,b_2] & \sigma_{b_3}^2 & \cdots \\ \vdots & \vdots & \vdots & \ddots \end{bmatrix}$$

$$\mathrm{Var}[\boldsymbol{b_c}] = \begin{bmatrix} \sigma_{c_1}^2 & 0 & 0 & \cdots \\ 0 & \sigma_{c_2}^2 & 0 & \cdots \\ 0 & 0 & \sigma_{c_3}^2 & \cdots \\ \vdots & \vdots & \vdots & \ddots \end{bmatrix}$$


[1] George, A., F. Seber, and C. J. Wild. "Nonlinear regression." (2003).
[2] Yang, Jia, Elbara Ziade, and Aaron J. Schmidt. "Uncertainty analysis of thermoreflectance measurements." *Review of Scientific Instruments* 87.1 (2016): 014901.
[3] Walpole, Ronald E., et al. *Probability and Statistics for Engineers and Scientists , 9th.* Vol. 6. Pearson, January, 2011. Chapter 4.1 & 4.2.
[4] Myers, Raymond H. *Classical and modern regression with applications.* No. 04; QA278. 2, M8 1990.. 1990. Chapter 3

# Other Density Measurement Techniques

**Grazing X-ray Reflection [1]**
- Sample roughness < 2 nm RMS
- Growth interface must be atomically smooth

**Rutherford Backscattering [3,4]**
- High energy ions (2.0 MeV $He^{2+}$)
- Destructive

**Spectral Ellipsometry [2]**
- Sample roughness < 10 nm RMS
- Optically transparent at probing wavelengths

**Ion polished SEM cross-section**
- 2D measurement
- Sample can melt during ion-polishing

[1] Toney, M.F., Brennan S., (1989). Structural depth profiling of iron oxide thin films using grazing incidence asymmetric Bragg x-ray diffraction. *Journal of Applied Physics*, **65**(12), 4763.
[2] Morral, A.F., Cabarrocas, P. R. (2004). Structure and hydrogen content of polymorphous silicon thin films studied by spectroscopic ellipsometry and nuclear measurements. *Physical Review B*, **69**(12), 125307.
[3] Jo M-H., Hong, J-K., Park H-H., Kim, J-J., Hyun, S-H. (1997). Evaluation of SiO2 aerogel thin film with ultra low dielectric constant as an intermetal dielectric. *Microelectronic Engineering*, **33**, 343-348.
[4] Samuelsson, M., Lundin, D., Jensen, J., Raadu, M.A., Gudmundsson, J.T., Helmersson, U., (2010). On the film density using high power impulse magnetron sputtering. *Surface & Coating technology*, **205**, 591-596.

2019-10-15- Coating -2-Gold-Indomethacin-Silicon–1229-Indo-10um-Si–Fit-Type-2

$\rho\ Cp_{\ (2)} = 1.58 \pm 0.24,\ \sigma_p = 0.17\ ,\ \sigma_{\text{fit}} = 0.17$

$k_{(\perp,\ 2)} = 0.21 \pm 0.05,\ \sigma_p = 0.02\ ,\ \sigma_{\text{fit}} = 0.05$

$G_{(1)} = 6.66 \pm 0.61,\ \sigma_p = 0.45\ ,\ \sigma_{\text{fit}} = 0.4$

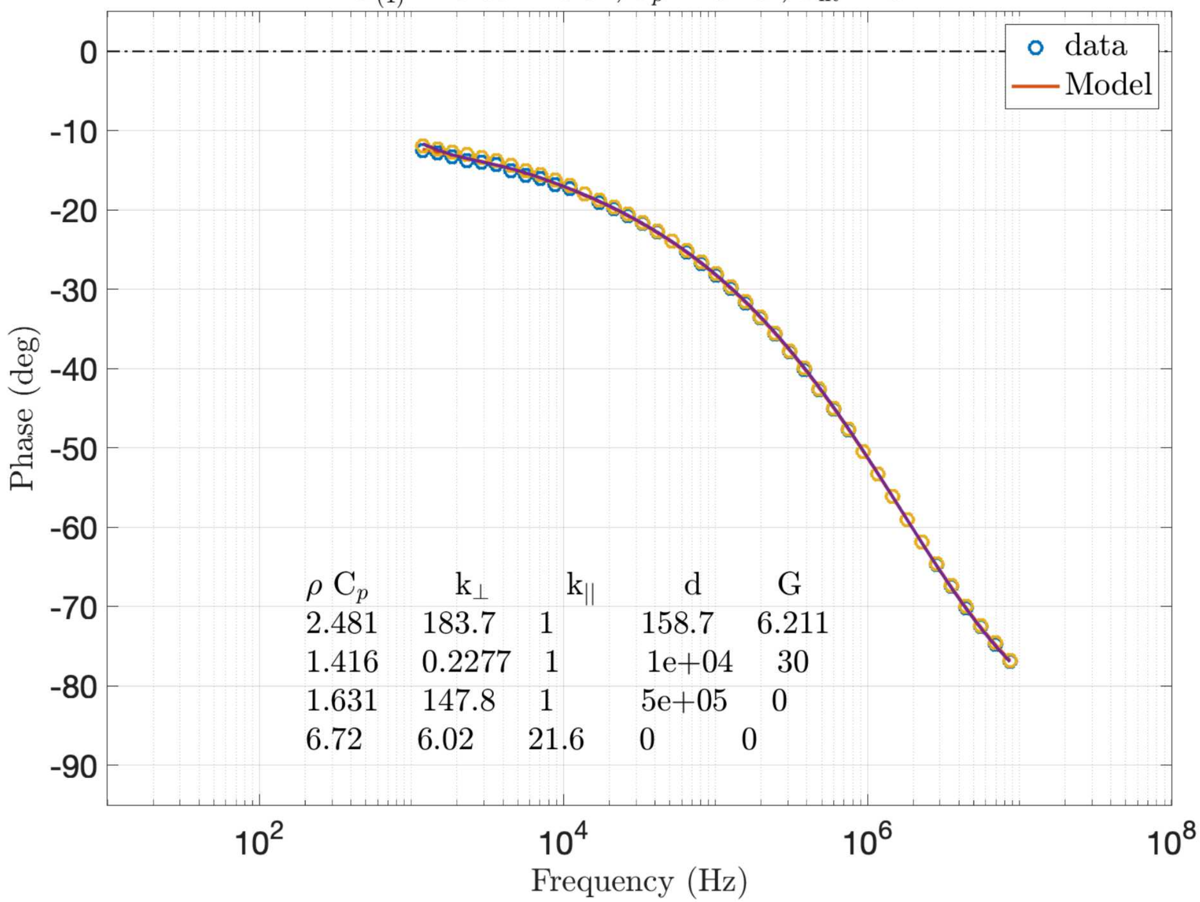


| | Thickness | | k cross 2 | | rhoCp | | Density | |
|---|---|---|---|---|---|---|---|---|
| | mean | std | mean | std | mean | std pop | mean | std |
| 1um SiO2 | 1040 | 55 | 0.16 | 0.02 | 1.52 | 0.038 | 1305 | ± 33 |
| 1um Si | 1080 | 170 | 0.18 | 0.048 | 1.55 | 0.011 | 1330 | ± 9 |
| 10um Si | | | 0.21 | 0.05 | 1.58 | 0.17 | 1356 | ± 146 |
| 100um Si | | | 0.18 | 0.04 | 1.64 | 0.076 | 1408 | ± 65 |

# Encased Low-k Films

| FDTR | Density (kg/m^3) | | percent of bulk | |
|---|---|---|---|---|
| | mean | std | mean | std |
| T1_09 (High) | 1760 | ± 269 | 99% | ± 15% |
| T3_08 (low) | 1630 | ± 148 | 92% | ± 9% |
| | | | | |
| C1_23 (low) | 1565 | ± 287 | 88% | ± 18% |
| C5_04 (low) | 1621 | ± 213 | 91% | ± 13% |
| C5_01 (hgih) | 1732 | ± 222 | 97% | ± 13% |
| | | | | |
| Gravimetric | Density (kg/m^3) | | percent of bulk | |
| | mean | std | mean | std |
| Nominally High | 1749 | 18 | 98% | |
| Nominally low | 1568 | 16 | 88% | |

End